universität wien

MASTERARBEIT/MASTER'S THESIS

Titel der Masterarbeit / Title of the Master's Thesis

Soil moisture content and its influence on urban climatology in the coupled model WRF-TEB during a heatwave in Vienna

verfasst von / submitted by

Kristofer Hasel, BSc

angestrebter akademischer Grad / in partial fulfilment of the requirements for the degree of

Master of Science (MSc)

Wien, 2020 / Vienna, 2020

Studienkennzahl lt. Studienblatt / degree programme code as it appears on the student record sheet:	UA 066 614
Studienrichtung lt. Studienblatt / degree programme as it appears on the student record sheet:	Masterstudium Meteorologie
Betreut von / Supervisor:	Assoc. Prof. Dr. Herbert Formayer

Contents

List of Tables

List of Figures

Abstract

The presentation of results from the urban climate project Urbania initiated some confusion on the customer side and resulted in a lively discussion about the interpretation of presented mean daily maximum temperature at 2 m over alluvial forests of the Nationalpark Donauauen. The presented temperatures showed the same values in areas of alluvial forests as in the city of Vienna. This work's aim is to find a concept for more accurate results regarding the climatology of forests and irrigated cropland in the greater Vienna area. This goal is realised by modifying the soil moisture content which is used in the initialisation of the model. Seven scenarios with different objectives are created with modifications in their soil moisture content in different layers according to the root length of the obtaining land cover. The model's maximum sensitivity could be shown with a reduction of 2.8 °C in the mean maximum of the mean diurnal 2 m temperature and a reduction of 12.2 °C in the mean maximum of the mean diurnal skin temperature. The alluvial forest's connection to groundwater can be numbered with a reduction in the mean diurnal 2 m temperature of up to 0.5 °C in the forest. A new category for alluvial forests has been implemented with a reduced stomatal resistance, which yields in an additional reduction of 0.3 °C. A fictive scenario where all of the domain's cropland becomes irrigated and a real case irrigation scenario both show negligible effects to Vienna's inner city temperature though the outer districts experience a reduction in the mean daily 2 m temperature of up to 0.5 °C.

Zusammenfassung

Die Präsentation der Ergebnisse aus dem Stadtklimaprojekt Urbania sorgte auf Kundenseite für einige Verwirrung und führte zu einer lebhaften Diskussion über die Interpretation der vorgestellten mittleren 2 m Tageshöchsttemperatur über den Auwäldern des Nationalparks Donauauen. Die vorgestellten Temperaturen zeigten in den Auwäldern die selben Werte wie in der Wiener Innenstadt. Ziel dieser Arbeit ist es daher, ein Konzept für genauere Ergebnisse bezüglich der Waldklimatologie und bewässerten Ackerflächen der Simulationsdomäne Großraum Wien zu finden. Dieses Ziel wurde durch eine Modifikation des Bodenfeuchtegehalts realisiert, der für die Initialisierung des Modells verwendet wird. Sieben Simulationen werden erstellt, mit modifizierten Bodenfeuchtegehältern in den unterschiedlichen Bodenschichten, abhängig von der darüber liegenden Vegetation und den unterschiedlichen Intentionen. Die maximale Sensitivität des Modells konnte mit einer Reduktion von 2.8 °C im mittleren Maximum des Tagesgangs der 2 m Temperatur und einer Reduktion von 12.2 °C im mittleren Maximum des Tagesgangs der Oberflächentemperatur beziffert werden. Die Versorgung des Auwaldes mit Grundwasser zeigt eine Reduktion des mittleren Maximums im Tagesgang der 2 m Temperatur um bis zu 0.5 °C. Eine neue Kategorie für Auwälder mit einem reduzierten stomatalen Widerstand des Bestandes wurde eingeführt, was eine zusätzliche Reduktion von 0.3 °C zur Folge hat. Ein fiktives Szenario mit Bewässerung aller Ackerflächen der Domäne und ein reales Bewässerungsszenario zeigen vernachlässigbare Auswirkungen auf die mittlere tägliche 2 m Temperatur in Wiens Innenstadt. Allerdings erleben die Randbezirke eine Reduktion von bis zu 0.5 °C.

1. Introduction

1.1 Motivation

The effects of the physiology and morphology of urban regions on the surrounding atmosphere have been in the focus of researchers for many years (Oke, 1973; Tran et al., 2006). A rise in air temperature, that can be expected because of climate change (Kromp-Kolb et al., 2014), increases the thermal stress for people especially in urban regions. Numeric weather models such as the weather research and forecast model (WRF) have been used to get a better understanding of the effects a city has on the urban atmosphere (Miao et al., 2009). To include the effects of an urban canopy in the numeric weather simulation, several specific models have been developed (Masson, 2000; Martilli et al., 2002).

As the hardware that is used for these numeric simulations increases in performance, it is possible to use higher resolutions to get a better understanding of small-scale effects. Therefore, it is of great interest to use the best available static data to initialise the numeric weather model to minimise a possible bias from the beginning (Schicker et al., 2016; Trimmel et al., 2019).

To simulate different urban growth scenarios and their effects on the urban atmosphere of Vienna during past and future heatwaves WRF was coupled with the town energy balance model (TEB) (Trimmel et al., 2019). The simulations were run in three nested domains with a spatial resolution of 333 m in the third domain. Due to this high resolution, it was of interest to use state of the art landuse data which has been realised by implementing the Corine landuse data from 2012 produced by European Environment Agency (EEA) (2012).

Alluvial forests appear close to rivers like the Danube river flowing through Vienna and are characterised by periodically flooding and high groundwater layer which results in permanent availability of water for the vegetation in this area. Consequently, even during heatwaves, like the one Vienna experienced in August 2015, the transpiration of an alluvial forest does not stop while vegetation elsewhere is already forced to reduce its transpiration caused by the lack of available water.

The aim of this work is to investigate how alluvial forests are represented in WRF and how the model's input data can be modified to represent alluvial forests more appropriately. Furthermore, a way to irrigate the cropland around Vienna is developed and the impacts of this irrigation are presented and discussed.

1.2 Previous Work - URBANIA

The aim of the Urbania project was to show how different urban development scenarios affect the temperature distribution in Vienna with respect to climate change in an extreme heatwave scenario with a periodicity of 15 years. The results of this project intend to help the city's government to develop effective strategies to cope with the expectable increased stress level on Vienna and its inhabitants triggered by a growing population and increasing temperatures (Kromp-Kolb et al., 2014).

1.2.1 Project Setup

In order to achieve the project goals the mesoscale numeric Weather Research and Forecast Model (WRF, Skamarock et al. (2005)) with three nested domains at a resolution of 3.0 km, 1.0 km and 0.333 km was coupled with the Town Energy Balance Model (TEB, Masson (2000)) as described in greater detail in section 2.

The coupling of WRF with TEB allows for three different urban categories with different morphologies. To rely on up to date data with high spatial resolution regarding landuse, a combination of the Corine dataset (European Environment Agency (EEA), 2012) and high-resolution data regarding population growth provided by Vienna's government was used and modified as described in Schicker et al. (2016) and Pineda et al. (2004). The created data were used to create the three urban development scenarios named REF, OPT and SPR (Trimmel et al., 2019).

REF defines the reference scenario with respect to Vienna's current development status. OPT is the optimised city scenario where the best materials for buildings with regard to heat conduction and insulation are used. Roofs and walls are virtually painted white for optimal reflection of incoming solar radiation and an optimal areal usage for the city's expected growth until the year 2050 is considered.

The scenario SPR (sprawl) describes the same as the REF scenario, except that Vienna's population growth until 2050 and thus the building of new apartments is not controlled and handled by the city's government. Every former green area next to an existing building was changed to urban land use to manage the bigger population resulting in a sprawling city.

The model was run for a current 15 year extreme heatwave (hw15yACT) which happened from 05.08.2015 to 13.08.2015 and a future 15 year extreme heatwave (hw15yrSCE) representative for 2036 - 2065. The results in Figure 1 show that the OPT scenario reduces the mean nightly minimal 2 m temperature by up to 1.5 °C in comparison to REF, while the SPR scenario leads to higher temperatures in the areas of new urban land use. A reduction of the urban heat island effect can be identified for the OPT scenario in the present heatwave (hw15yACT) as well as for the future heatwave (hw15ySCE).

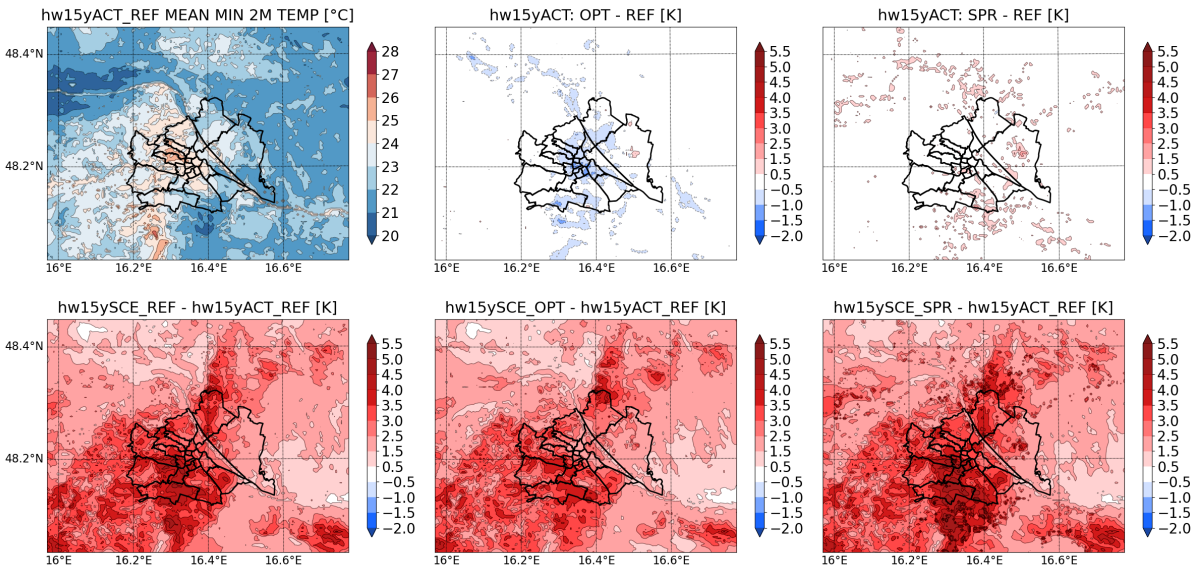

Figure 1: Daily mean minimum 2 m temperature of the selected cloud free days for the present heat wave hw15yACT (upper left). Differences between reference scenario hw15yACT and urban development scenarios OPT (middle) and SPR (right) (upper panels). Differences between reference scenario for present (hw15yACT) and future (hw15yrSCE) for the REF (left), OPT (middle) and SPR (right) urban development scenario (lower panels) (Trimmel et al., 2019).

1.2.2 Resulting Questions

Figure 2 was used by the Urbania project team to present their first results to the department of urban development of Vienna's government. The distribution of the daily mean maximum 2 m temperature caused some irritation on the customer's side because it is as hot in the alluvial forest of the Nationalpark Donauauen, framed by green contours in Figure 2, as it is in the city of Vienna. The same applies to the cropland around Vienna which seems to be even hotter than some parts of the city. Based on personal experience one would expect a reduced thermal stress on one's body when being in a forest, especially an alluvial forest.

This lively discussion was the initial spark for this master thesis. The interesting questions raised in this discussion will be dealt with in this work.

.

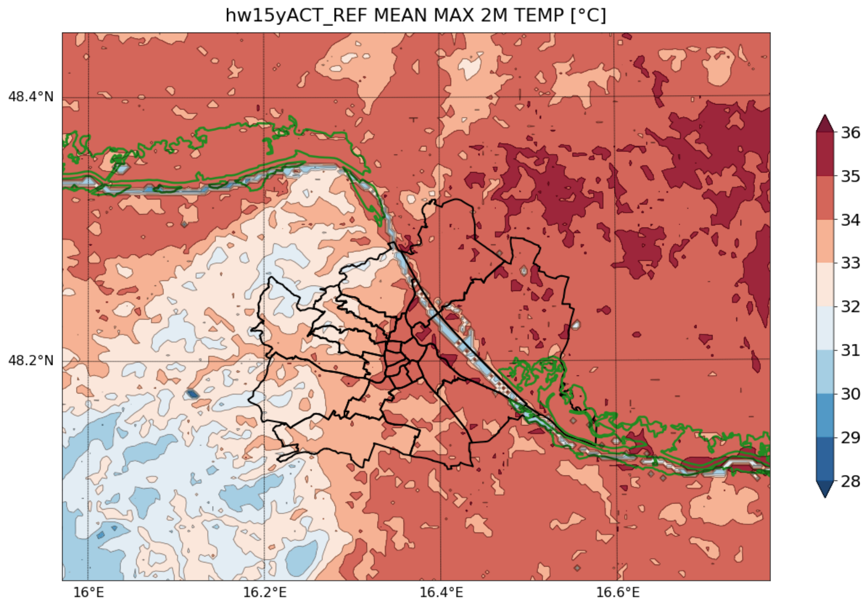

Figure 2: Daily mean maximum 2 m temperatue of the selected cloud free days for the present heat wave hw15yACT. The Nationalpark Donauauen is framed by green contours.

1.3 Research Questions

As mentioned above, the expected effects of alluvial forests and irrigated croplands cannot be seen in the results of the Urbania project. The missing effects caused by irrigation or the characteristics of an alluvial forest rise several interesting questions:

- How does the soil moisture content influence the 2m temperature and evapotranspiration?
- How can the initial soil moisture parameter be modified to elucidate the effects of irrigation or an alluvial forest?
- How will the modified soil moisture parameter affect the temperature in these areas?
- Will the created effects also influence the temperature in Vienna?
- Is it an improvement to create a new landuse category for alluvial forests?

2. The Coupled WRF - TEB Model

This chapter describes the structure and workflow of the WRF model and its containing NOAH land surface model as well as its setup for this work. The TEB model will be introduced and its coupling with WRF explained briefly.

2.1 Weather Research and Forecast Model (WRF)

WRF is an unitized open source mesoscale numerical weather simulation model developed by the National Center for Atmospheric Research (NCAR), the National Center for Environmental Prediction (NCEP), the Earth System Research Laboratory, the U.S. Air Force, the Naval Research Laboratory, the University of Oklahoma and the Federal Aviation Administration (FAA) (Skamarock et al., 2005). Due to its open source mindset and its modularity, a large professional community evolved who pushed its development further into various fields. It is used as a tool for analysing past events, as operational weather forecast model or as regional climate model just to name a few of the possible implementations (wan).

The WRF model offers two different options of dynamical solvers, referred to as the ARW core (Advanced Research WRF) and the NMM core (Nonhydrostatic Mesoscale Model). Both are non-hydrostatic and fully compressible, with the main difference being that the ARW Model offers more configuration options.

2.2 WRF Workflow

The content of this section is mainly taken from the WRF-ARW User Guide v 3.9 and Rausch (2012). The workflow of real data cases processed in this work is split up into two major programs as shown in Figure 3: The WRF Pre-Processing System (WPS) and the WRF Model itself. The modules OBSGRID and WRFDA are used to implement external observational data like radiosonde reports or radar data which are used for example in operational forecasts. As they are not used in the simulations of this work, they will not be explained further.

The WPS splits up into three subroutines: *geogrid*, *ungrib* and *meteogrid*.

Geogrid's main purpose is to interpolate the terrestrial, static data to the model grid according to a user-defined configuration file and save it to a netcdf file. The file includes latitude/longitude coordinates, soil categories, land use category, terrain height, annual mean deep soil temperature, monthly vegetation fraction, monthly albedo, maximum snow albedo, and slope category.
Ungrib takes time-varying meteorological data stored in GRIB files and writes these to a simple intermediate format.
Metgrid takes these intermediate files provided by ungrib and interpolates them horizontally to the simulation domain provided by Geogrid.

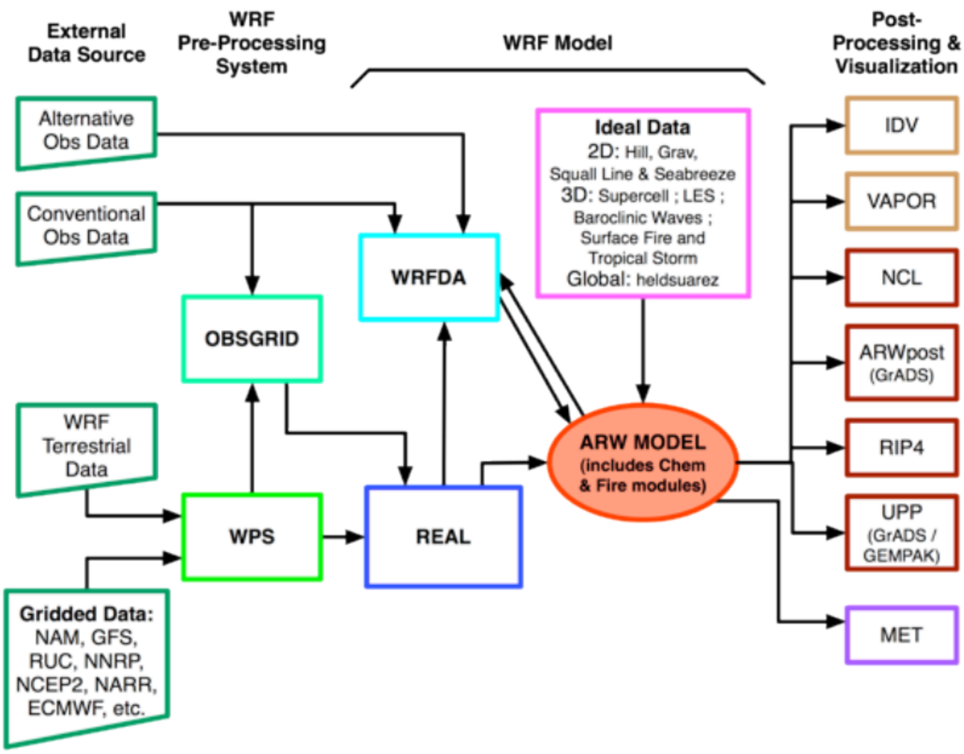

Figure 3: WRF workflow taken from WRF ARW Userguide v 3.9 (Mitchell, 2005)

The WRF Model splits up into two subroutines: *real* and *wrf*.

Real vertically interpolates the Metgrid output to the model's vertical coordinates, checks if the parameters provided by Metgrid are consistent and prepares the soil fields according to the selected land surface scheme. It then creates a lateral boundary condition file and a initialisation file for *wrf.exe* for the initialisation of **WRF**.

2.3 Setup

In this work WRFv3.9.1 (Skamarock et al., 2005) is used with the same configuration as in the Urbania project and shown in Table 1.

The model was run with three nested domains. The first domain has a 3 km spatial resolution and contains most of Austria (except for Tyrol and Vorarlberg), southern parts of Czech Republic, parts of Slovakia, Hungary and Slovenia, see Figure 4.
Domain two, with a spatial resolution of 1 km, focuses on Vienna and covers Lower Austria and parts of Northern Burgenland including the Neusiedlersee.

The third domain, with the highest resolution of 333.3 m, is centered on Vienna. It also covers Vienna's surrounding area including parts of the Wienerwald on the alpine foothills in the west, the alluvial forests around Tulln in the west and north of Vienna, the Naturpark Donauauen close to the Danube river in the Southeast of Vienna and the mostly agriculturally used Marchfeld in the east. South and north of the domain, a mixture of agriculture and industrial land cover prevails.

Table 1: Physical scheme configuration for WRF-TEB used in the Urbania project and this work.

Term	WRF Shortname	Scheme Name
Microphysics	*mp_physics*	WRF Single-Moment 6-class scheme
Cumulusphysics	*cu_physics*	OFF
Longwave Radiation	*ra_lw_physiscs*	RRTMG scheme
Shortwave Radiation	*ra_sw_physics*	RRTMG shortwave
Planetary Boundary Layer	*bl_pbl_physics*	Mellor-Yamada-Janjic scheme
Surface Layer	*sf_sfclay_physics*	Eta similarity
Land Surface	*sf_surface_physics*	NOAH Land Surface Model
Urban Surface	*sf_urban_physics*	TEB

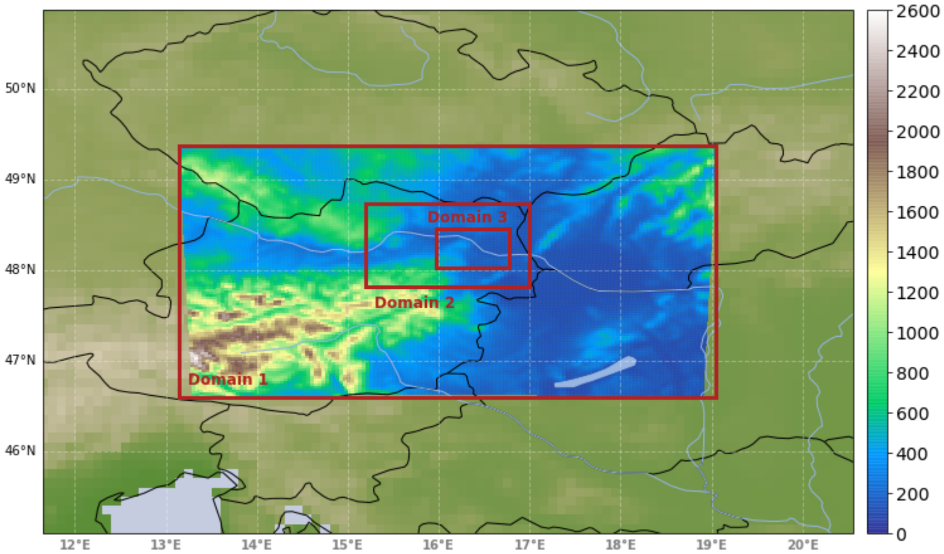

Figure 4: Nested WRF domains with 3 km, 1 km and 333.3 m spatial resolution. Also shown the model height of domain one in m created with SRTM and preprocessed by WPS.

The third domain's altitude varies from 140 m to 615 m whereas the altitude in Vienna itself varies between 140 m and 542 m with the lowest point located in Lobau and its highest point at Hermannskogel.

As we are only interested in days without any interference caused by clouds, WRF's "downward solar radiation on surface", *SWDOWN*, variable was used to determine cloud free days. Hence, the days *08.08.2015, 09.08.2015* and *12.08.2015* were identified to not show any clouds in both the simulation and reality, and are thus used for further calculations.

2.4 WRF NOAH Land Surface Model

The NOAH Land Surface Model simulates surface energy and moisture fluxes as well as surface energy and moisture budgets and their interaction with the first layers of the atmosphere (Ek et al., 2003).

It is a 1-D column model with predefined landuse and soil categories. The landuse category's properties are stored in the *VEGPARM.TBL* table file with respect to winter or summer. The soil is divided into four layers where every layer can have different properties according to its material composition. The division into four layers allows to consider variable root lengths for different vegetation types which has an impact on the calculation of evapotranspiration. Different soil compositions and their properties like maximum soil water content are predefined and stored in the *SOILPARM.TBL* table file.// With the just described information the NOAH land surface model calculates the land surface's skin, soil temperature and turbulent fluxes which are in exchange with the atmosphere above.

2.4.1 NOAH Land Surface Model Workflow

The following list provides an overview of the NOAH land surface model's main workflow. The workflow of the most important part in the model, the calculation of the meteorological relevant fluxes that are in exchange with the atmosphere, will be described in more detail in the following subsection *Physics routines (KEY CALL)* (Mitchell, 2005).

- Read control file including land surface model (LSM) initial conditions and site characteristics.
- Begin of optional multi-year spin-up loop if invoked by control file (optional).
- Begin of time step loop.
    * Read atmospheric forcing data and observed validation variables.
    * Interpolate monthly albedo and vegetation greenness to current julian day.
        · Determine julian day for current time.
    * Calculate actual and saturated specific humidity.
        · Calculate vapor pressure.
    * Calculate slope of saturation specific humidity with respect to air temperature (needed in PENMAN)
    * Call to family of physics routines (**KEY CALL**).
    * Write output.
- End of time step loop.
- End of optional multi-year spin-up loop.

Physics routines (KEY CALL)

The most import part of the NOAH land surface model, the call of the physics routines, is summarised in the following list. These routines calculate and update the variables that are in interaction with the atmosphere.

- Set land-surface parameters like soil type or landuse category.
- Set soil type dependent parameters like wilting point, maximum and minimum of possible soil moisture content (parameters are defined in table file *SOILPARM.TBL*).
- Set vegetation type dependent parameters like Leaf Area Index or stomatal resistance (parameters are defined in the table file *VEGPARM.TBL*).
- Update snow depth and snow density to account for new snowfall.
- Determine snow cover fraction.
- Determine surface albedo (including snow cover fraction).
- Compute soil thermal diffusivity.
- Compute snow roughness length.
- Calculate surface exchange coefficient for heat/moisture.
- Compute potential evaporation.
- Compute canopy resistance.

After this initial steps there are two pathways which depend on either (1) it is snowing or (2) if there already is an existing snowpack or (3) if it is too warm for snow. Those two paths only differ in the consideration of the snow layer in the surface energy balance and the additional calculation of the snow depth.

As a heatwave is being examined in this work, only the second pathway without snow is relevant and will be presented.

- Update surface skin temperature via surface energy balance.
- Compute surface water fluxes and layer soil moisture content.
  - Compute direct evaporation from top soil layer.
  - Compute transpiration from vegetation canopy.
  - Compute time-rate-of-change of soil moisture.
    - Compute hydraulic conductivity and diffusivity.
  - Forward time-step integration of soil moisture rate-of-change.
- Compute soil thermal diffusivity.
- Compute ground heat flux and layer soil temperature.
  - Compute time-rate-of-change of soil temperature.
    - Compute soil thermal diffusivity (dependent on soil moisture).
    - Determine soil layer interface temperature.
    - Compute heat sink/source from soil ice phase change.
      - Compute soil thermal diffusivity.
      - Calculate subzero unfrozen soil water.
    - Forward time step integration of soil temperature rate-of-change.

2.4.2 Calculation of 2 m Temperature (T2)

The temperature at 2 m is a common variable in the WRF output and is measured by weather stations built according to the regulations defined by the World Meteorology Organisation (WMO). As already mentioned in Section 1, the mean maximum 2 m temperature in the alluvial forest shown in Figure 2 does not represent the real climatology of a forest, described in Section 4.6. It is thus interesting to know how this temperature is calculated in WRF.

As the 2 m temperature is not on a vertical model level WRF has to determine it separately. This is not done by the NOAH land surface model because the 2 m temperature is independent of the used land surface scheme. Instead it is calculated in the module for surface diagnostics named *module_sf_sfcdiags.F* which also calculates the 2 m relative humidity as well as the 2 m potential temperature.

$$T2 = TSK - \frac{HFX}{\rho \cdot c_P \cdot CHS2} \tag{1}$$

Equation 1 shows the calculation of the 2 m temperature $T2$ in Kelvin with TSK being the skin temperature in Kelvin, HFX the sensible heat flux in W/m^2, ρ the density of air in kg/m^3, c_P the specific heat capacity at constant pressure with 1004.5 J/kgK and $CSH2$ the thermal conductivity at 2 m in m/s.
Except for c_P all variables get updated or calculated in the surface layer scheme which in this work is the NAOH land surface model.

2.5 Town Energy Balance Model (TEB)

Land surface models, such as NOAH, simulate the interaction between atmosphere and land surface in a simplified way because the land surface is a plain two dimensional field with defined properties. This is valid for all kinds of land covers like crops, woods and also urban areas. The simplification to a two dimensional plane may work for simulations on a synoptic scale or a bigger meso-scale, but with increasing spatial resolution much of the small scale interactions and information are lost (Meyer et al., 2020).

The TEB Scheme is designed for urban surface parametrisation and follows a one layer canyon approach. This canyon approach is again simplified by two facing walls, a roof and a road but allows to simulate the energy budget for those three sub layers. This then allows for effects like partly trapped solar radiation which is crucial for effects like the urban heat island (UHI).
In general, TEB aims to simulate the turbulent fluxes in the urban canyon and therefore parameterises the urban surface and the roughness sublayer so that the coupled atmospheric model, in this work's case WRF, only sees a constant flux layer at its lower boundary (Masson, 2000; Masson et al., 2002).

In 2012, the Building Energy Model (BEM) was added to TEB which, for example, allows to take into account the energy effects of buildings and their influence on urban climate.

Furthermore, it delivers the possibility to estimate the building energy consumption of the city (Bueno et al., 2012). Additionally, road orientation and a separated energy balance of adjacent walls were added to TEB as well as gardens (Lemonsu et al., 2012).

A Greenroof Model was implemented into TEB in 2013 by De Munck et al. (2013). This model aims to simulate the interaction between building roofs and various greenroof systems and shows their effects on urban climate.

The option for solar panels was added by Masson et al. (2014) and shows a reduced urban heat island effect. Human behaviour and their impact on building energy consumption is shown by Schoetter et al. (2017)'s parametrisation. With the latest improvement by Goret et al. (2019) even CO_2 fluxes can be calculated with TEB.

2.5.1 Coupling WRF with TEB

In general, TEB is either used in offline mode or coupled with other land surface models. For the Urbania project, TEB was coupled with WRF's NOAH land surface model. The procedure is following the generalised coupling methodology introduced by Best et al. (2004) to improve the calculation of surface fluxes and can be briefly described by the following workflow (Meyer et al., 2020):

- WRF provides meteorological data like wind or radiation from the lowest model level as well as static data like grid cell coordinates. Surface parameters (e.g. building height) are provided by WRF via the look up table *URBPARM.TBL* as input for TEB.
- With this information, TEB computes area averaged surface quantities like the sensible heat flux and passes them back to WRF.
- Surface diagnostics (e.g. building energy consumption or building power demand for cooling) are calculated in TEB and passed to WRF as output without interfering with the calculations in WRF's dynamical core.

TEB's code of the coupled WRF-TEB model is only active for the domain's urban areas. The interaction between land surface and atmosphere of all other categories is still handled by the NOAH land surface model only (Meyer et al., 2020).

3. Data

Since the third domain has a high resolution of 333 m, it is necessary to use data in a similar or even higher resolution. Coarser data can not provide the same amount of information and can have a negative influence on the results (Schicker et al., 2016).

By now a lot of the data are freely available and can easily be downloaded from the internet. The data used in this work are described in this chapter.

3.1 Shuttle Radar Topography Mission (SRTM)

NASA's Shuttle Radar Topography Mission was started in 2000 in collaboration with the National Geospatial-Intelligence Agency and the German and Italian Space Agencies and represents the global topographic data with the highest resolution (Farr et al., 2007). The global dataset was released to the public in late 2015. Its resolution is one arc-second which is about 30 m.

3.2 Copernicus Corine Land Use clc2012

The Corine land cover dataset clc2012 was produced by the Copernicus program of the European Environmental Agency (EEA) and is based on photointerpretation of satellite images. It is available for almost all of Europe, updated every 6 years and freely accessible (European Environment Agency (EEA), 2012).

In the case of the clc2012 dataset, the IRS P6 LISS 3 and RapidEye satellite data were used. A overview about the properties of the clc2012 Corine land cover dataset is listed in Table 2.

Table 2: Properties of clc2012 Corine land cover dataset.

Resolution	≤ 100 m
Geometric Accuracy	≤ 25 m
Thematic Accuracy	≥ 85 %
Time Consistency	2011 – 2012
Landuse Categories	44

To generate different scenarios, the Corine land use data was modified as described in Section 4.5.

3.3 Integrated Nowcasting through Comprehensive Analysis System (INCA)

To evaluate the initial situation of WRF-TEB's simulations, the results will be compared to INCA data (Haiden et al., 2011) produced by the Zentralanstalt für Meteorologie and Geodynamik (ZAMG). It is a multivariable analysis and nowcasting system that was developed especially for mountainous regions. To create the analysis fields, the system combines surface station data, remote sensing data and ALADIN's numerical weather prediction data (Wang et al., 2006). The numerical input data are not limited to ALADIN, the Swiss version of INCA for example uses data produced by COSMO as a first guess (Steppeler et al., 2003).

The algorithm works in such a way that the observational data at the surface station locations will be reproduced and the remote sensing data and numerical weather prediction data deliver the structure between the stations for interpolation (Haiden et al., 2011). Table 3 gives an overview about INCA's general features in the Austrian domain.

Table 3: Properties of INCA's dataset used in the Austrian domain.

Description	Parameter	Value
Spatial Resolution	all	1 km
Temporal Resolution	Temperature, Humidity, Wind, Global Radiation, Snowfall line, Ground Temperature	1 h
	Precipitation, Precipitation Type, Cloudiness	15 min

3.4 ECMWF Operational Analysis

To meet WRF's need for boundary conditions, European Center for Medium-Range Weather Forecast's (ECMWF) operational analysis data is used (ECMWF, 2018). It is a global dataset and available in ECMWF's original latitude/longitude grid with ECMWF's highest resolution of 0.1° and a 6 h frequency.

All parameters for the boundary conditions were used from this dataset except for soil moisture. In this case, the assimilated soil moisture of the Global Land Data Assimilation System (GLDAS) Noah land surface model v2.1 is used, described in Section 3.5.

3.5 GLDAS Noah Land Surface Data - Soil Moisture

As the soil moisture content has a big impact on the land surface and atmosphere interaction fluxes, it is, especially for high resolution simulations, mandatory to use as accurate data for soil moisture as possible (Hirschi et al., 2011; Schicker et al., 2016; Greve et al., 2013).

The GLDAS Noah land surface model operates three offline (not coupled to the atmosphere) land surface models, to generate fields for land surface states like soil moisture. To do so, it ingests satellite- and ground based observational data and uses advanced land surface modeling and data assimilation techniques to produce the required fields on a global scale (Rodell et al., 2004). Table 4 gives a short overview on GLDAS's data properties.

Table 4: GLDAS Noah land surface model's general properties.

Spatial Resolution	0.25°
Temporal Resolution	3 h
Land Surface Models	Noah-3.6, CLSM-F2.5, VIC-4.1.2

3.6 Agricultural Risk Information System (ARIS)

The Agricultural Risk Information System (ARIS) was developed as part of the Agro Drought Austria (ADA) ACRP project. Its main goal is to monitor the available soil moisture content and forecast potential dry periods for different agricultural crops like winter wheat or maize in a high resolution (see Table 5).

Table 5: General properties of ARIS's soil data.

Spatial Resolution	500 m
Temporal Resolution	daily
Short- and Midterm Forecast Length	10 days

Based on the existing models SpatialGRAM and SOILCLIM, ARIS uses information about the soil, vegetation characteristics and meteorological data to calculate crop drought and heat stress indicators. Its aim is not only to support farmers in planing and coordinating their production cycles, but also to deliver important information to for example insurance companies and the general public (Eitzinger et al., 2016).

The produced fields can be viewed via the GIS web application at `https://warndienst.lko.at/trockenheit+2500++1071890` (last accessed 03.06.2020).

To be able to compare the data with the WRF-TEB results, the soil moisture content of the top 0 - 40 cm and bottom 40 - 100 cm layer was made available as netcdf files by Josef Eitzinger and Gerhard Kubo of the University of Agriculture and Lifesciences, Department of Meteorology. The data only covers agriculturally used areas of Austria.

4. Methods

In this chapter properties of the generated simulations and preprocessing of the data used in WRF-TEB are described. WRF's initialised soil moisture content for the first two layers is compared to soil moisture calculated by an agricultural model. Finally, the model's simulation result for the 2 m temperature of the reference scenario REF is compared to INCA.

4.1 Heatwave August 2015

August 2015 was the 4^{th} hottest August since the beginning of meteorological records at the Zentralanstalt für Meteorologie und Geodynamik. Starting with the 4^{th} of August a heatwave hit Austria with daily maximum temperatures exceeding 35 °C for 9 days in a row. What makes this event so special is that up to this heatwave the record for days exceeding 35 °C counted over the whole year, had been 5 days in Vienna (`https://www.zamg.ac.at/cms/de/klima/klima-aktuell/klimamonitoring/`).

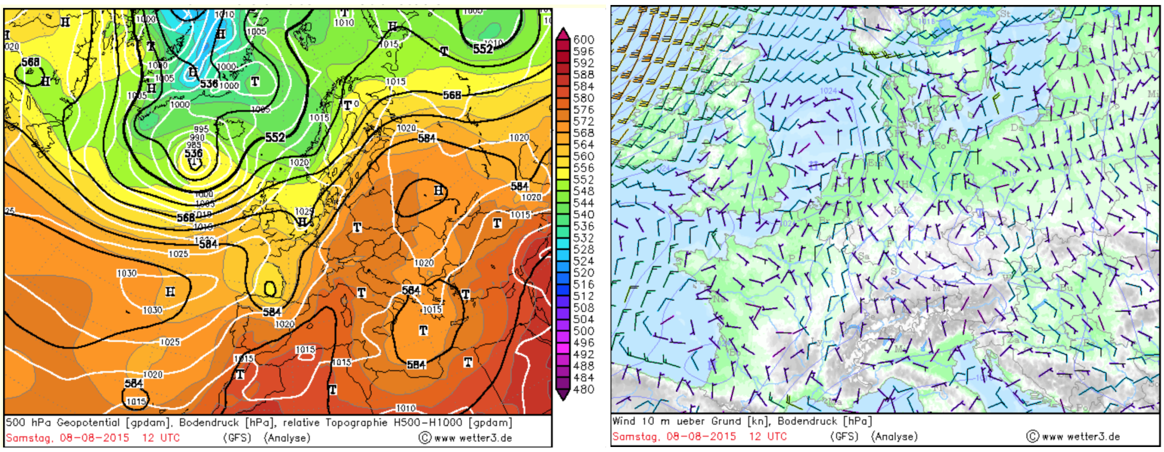

Figure 5: Surface pressure over Europe in hPa (white contours), 500 hPa geopotential (black contours) and relative topography (filled contours) in the left plot and 10 m wind speed and direction in the right plot for the 08.08.2015 12 UTC during the heatwave in August 2015. Figures taken from `http://www1.wetter3.de/`.

Over Central Europe a high-pressure system stretches from the Eastern part of Russia to southern part of Spain. This connects to another strong high pressure system over the Atlantic Ocean west of France and Spain relating there to very low wind speeds, shown in Figure 5. Southwest of Iceland there is a low-pressure system which causes strong winds in Ireland and north of Great Britain.

Figure 6 shows the daily mean temperatures for August 2015 for the TAWES station Wien Hohe Warte, clearly indicating the heatwave from 5^{th} to 16^{th} of August 2015. The thin lines above and below the climatological mean are the measured maximum and minimum daily

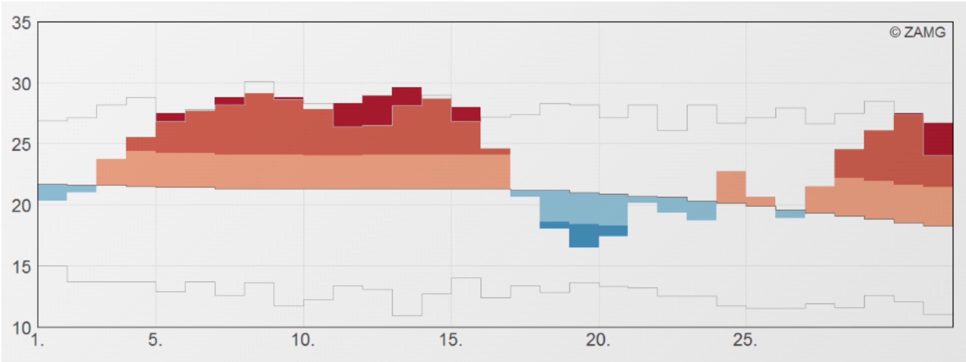

Figure 6: Climate Monitoring for TAWES station Wien Hohe Warte (taken from `www.zamg.ac.at/`*). Red marks daily mean temperatures above the climatological mean related to 1981 - 2010 while blue marks temperatures below the climatological mean. Thin lines show the absolute minimum or maximum measured on that day of the year.*

mean temperature measured in the past for that particular day. Only within this time period six new daily maxima were measured, marked by the dark red colour on top.

4.2 Comparison of WRF-TEB with INCA

As already described in Section 3.3, INCA is used to evaluate the initial situation of the WRF simulation. Since INCA data differs from our WRF output in terms of grid resolution and position it has to be regrided to the WRF domain three. This was done with the python *xesmf* package (`https://xesmf.readthedocs.io/en/latest/`). The algorithm *nearest neighbour* was used because it is monotonic and does not create new maxima or minima.

With both data sets on the same grid and with the same resolution the diurnal temperature at 2 m was calculated and compared for the whole domain three and the three defined cloud free days. As can be seen in Figure 7's left plot, the diurnal's cycle mean maximum temperature during the day agrees reasonably well with the WRF temperature and is only lower by 1 °C in the mean maxima. The mean minimum temperature during nighttime shows a bigger difference with the INCA temperature being 3 °C lower than WRF. This is also reflected in the right plot of Figure 7 where the linear regression shows a difference in the lower temperatures towards the REF axis. No grid point of the domain reaches a temperature below 20 °C while the mean minimum of the INCA data is around 17 °C. Except for the difference in the mean minimum the 2 m temperature's diurnal circle is well reproduced.

Figure 8 shows the difference in the mean 2 m temperature for the selected cloud free days. The southern and mostly industrial part of Vienna shows a difference lower than 0.5 °C while the rest of Vienna and also the mostly agriculturally used area around Vienna reveal differences between 0.5 °C and 1.5 °C. The described comparison above and the calculated coefficient of determination R^2 of 0.94, shown in Figure 7's left plot, indicate that the WRF-TEB model captures the simulated heatwave from 05.08.2015 to 13.08.2015 and its distribution of the 2 m temperature comprehensible and well.

The differences illustrated in Figure 8 are to be expected because the resolution of the WRF-TEB model is three times higher than the INCA's model resolution. Also, as mentioned in Section 3.3, INCA only considers observations from stations and interpolates the parameters inbetween with the help of the output of a numerical weather prediction model or radar data or for the 2 m temperatures only with a fingerprint for the topography and the gradient between the observation stations. Hence, it does not consider the underlying land use category which usually affects the meteorological parameters that the model is computing on a finer scale.

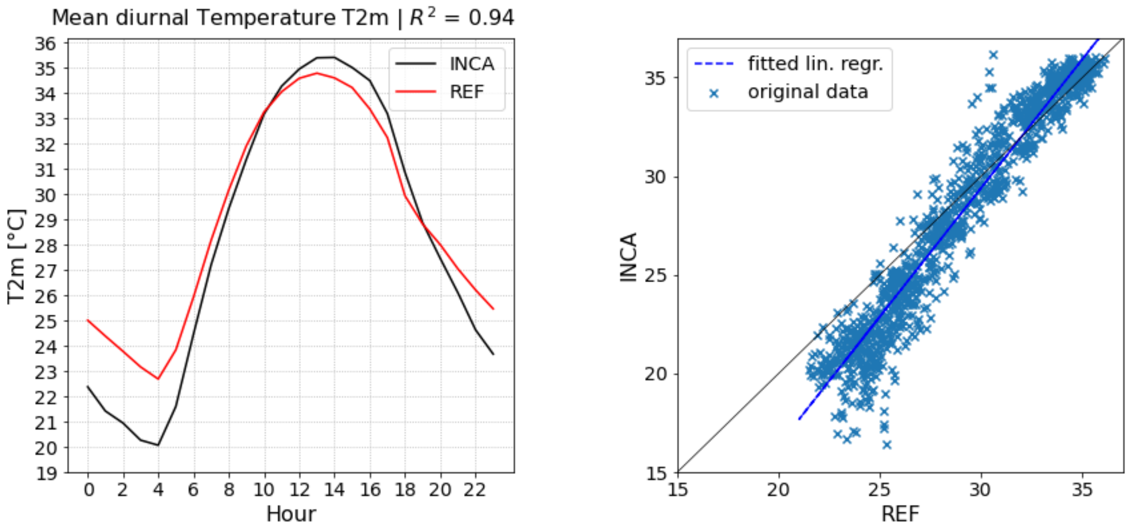

Figure 7: Comparison for 2 m temperature between INCA and WRF-TEB's REF simulation. On the left the 2 m temperature's diurnal circle for the selected cloud free days, on the right a plot with INCA data on the y- and REF data on the x-axis.

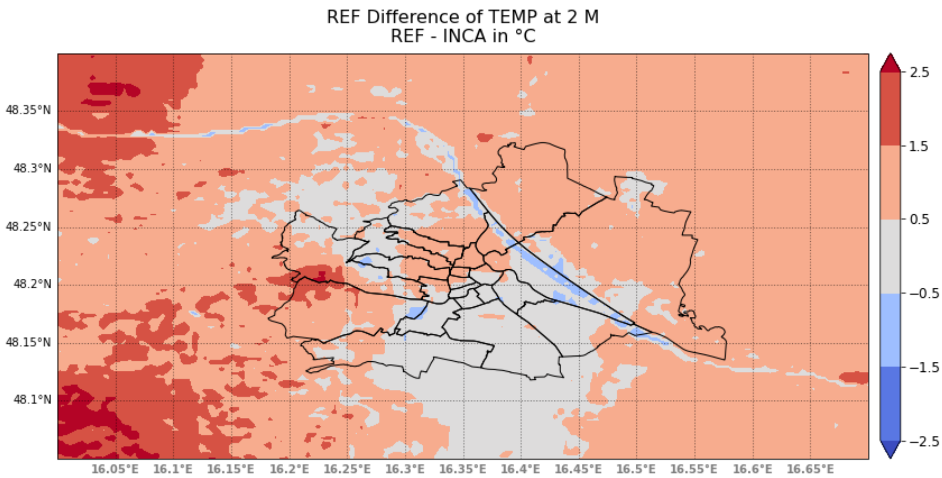

Figure 8: Difference in mean 2 m temperature between INCA and WRF-TEB's scenario REF for the defined cloud free days 08. / 09. / 12.08.2015 during the heatwave of August 2015.

4.3 ARIS Comparison with WRF-TEB

As described in Section 3.6 the soil moisture data of ARIS has a spatial resolution of 500 m. Consequently, in a first step, it has to be regrided to the third WRF-TEB domain's resolution of 333 m. This was realised with the python *xesmf* package using the conservative *nearest neighbour* algorithm. The algorithm is called conservative because it is not creating new maxima or minima in the regrided data.

The soil moisture content of WRF-TEB's NOAH model is initialised and calculated for four layers: 0 - 10 cm, 10 - 40 cm, 40 - 100 cm and 100 - 200 cm. The first two layers are added up according to Equation 2 in order to be able to compare it to ARIS (the data only has two layers from 0 - 40 cm and from 40 - 200 cm).

$$SMC_{a+b} = \frac{SMC_a * h_a + SMC_b * h_b}{h_a + h_b} \tag{2}$$

The indices a,b represent the different layers while the variables h_a, h_b define the height of these layers. In this context the index a+b defines the newly calculated layer.

As ARIS's data have a daily temporal resolution, the hourly resolution of WRF-TEB's data was resampled to daily values. With the data on the same grid, the same layer depth and the same temporal resolution 08.08.2015, the first day of the selected cloud free days, was chosen to calculate the difference between WRF-TEB and ARIS.

Figure 9 shows that even though the already preprocessed GLDAS data were used, the WRF-TEB soil moisture content is generally too high. Only in the north of Vienna ARIS data are wetter than WRF-TEB because it probably rained in this area in the previous days.

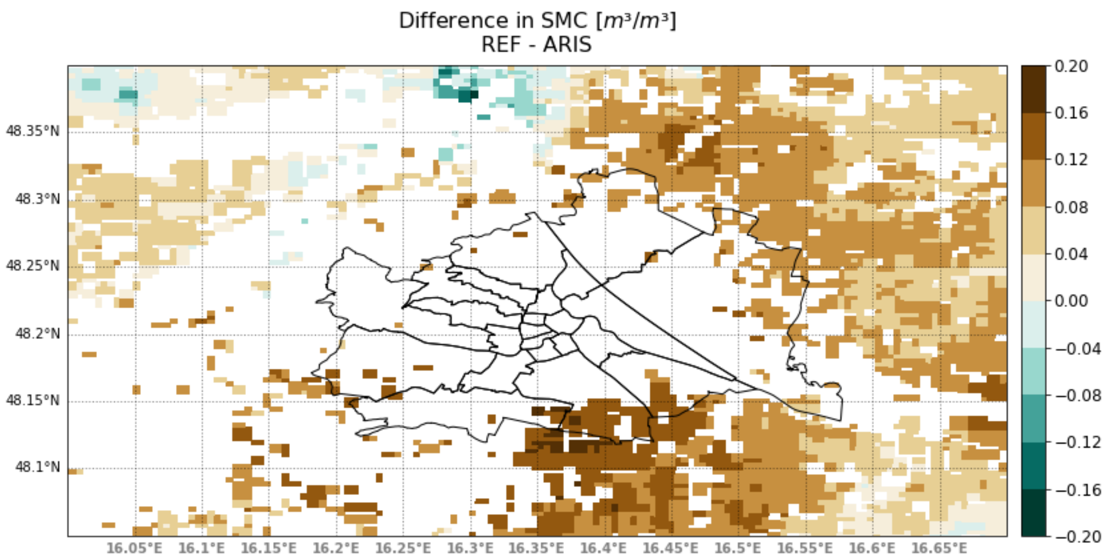

Figure 9: Difference in soil moisture content (SMC) in the top layer 0 - 40 cm between WRF-TEB's reference scenario REF and the soil moisture content produced by ARIS for 08.08.2015.

4.4 Soil Moisture

Soil moisture is a crucial factor in the distribution of surface energy fluxes. Equation 3 describes the surface energy balance with F as the net radiation , H_S as the sensible heat flux, H_L as the latent heat flux and H_G as the ground heat flux (all in W/m^2). If the moisture increases, described by the specific moisture q in equation 4, the latent heat flux will increase. Consequently, as Equation 3 is a statement of balance, the sensible heat flux H_S decreases as the incoming radiation energy is used to evaporate the moisture. L in Equation 4 is the latent heat of vaporization with 2.464 MJ/kg, ρ the air's density in kg/m^3 and v the velocity in m/s (Oke, 1973).

$$F + H_S + H_L + H_G = 0 \tag{3}$$

$$H_L = \rho * v * L * q \tag{4}$$

In the context of climate change not only the mean temperature is about to rise (Kromp-Kolb et al., 2014). Studies indicate that there will also be a higher variability meaning that extreme events will occur more frequently and even more severe (Klein Tank and Können, 2003).

The observational study performed by Hirschi et al. (2011) indicates an increased occurrence of droughts with increased duration for south east Europe because of decreasing soil moisture content. It also agrees with model results which showed an amplification of temperature extremes in the context of global warming linked with geographical soil moisture regimes for Europe.
A change in atmosphere-land coupling is significantly affected by global warming as a northwards shift of the climatic zones appears. Thus a new transitional zone between dry and wet climate is being established in central and south east Europe (Seneviratne et al., 2006).

4.5 Preparation of clc2012 Corine Landuse

The Corine clc2012 dataset is used to maintain an accurate and up-to-date land cover classification and is available as a raster geotiff file. As WRF only works with its predefined landuse classification datasets like USGS and Modis, the clc2012 data has to be reclassified in order to be used. This is done according to Pineda et al. (2004) who created a transformation table between USGS, Modis and Corine.

As WRF's preprocessing model WPS only accepts static geographic input data in binary format, the data is converted with the commandline utility *convert_geotiff* (`https://github.com/openwfm/convert_geotiff/`) which was developed by the WRF wildland fire modeling community (WRF-Fire,
`https://www.openwfm.org/wiki/Open_Wildland_Fire_Modeling_E_community_Wiki/`).
The utility uses WRF's own *read_geogrid.c* and *write_geogrid.c* C-routine and works in the same way as described in Chapter 3-39 of WRF's User Guide but in a handier way that al-

lows an easy change of options like tile border size or file size. The index file which contains information needed by WPS is created automatically in the process.

Additionally a new category "alluvial forest" is created. This was done by adding the category to the *VEGPARM.TBL* file and also set the designated areas of the domain to this category. The parameters of the category are the same as the USGS category 11 "deciduous broadleaf forest" but with a reduced stomatal resistance RS of 60 1/m instead of 100 1/m. Consequently a higher evapotranspiration for this category is expected.

4.6 Forests

Forests show a different climate compared to an open field or cropland. The biggest difference one notices when walking through a forest is the decreased temperature. This is not only caused by shading, but also by increased evapotranspiration. Figure 10 shows the usual mean diurnal temperature distribution in a young spruce forest. During nighttime the temperature is nearly isothermic while its daily maximum can be observed near the treetops. At midday a difference in temperature between ground and treetop of about 6 °C develops (Schume, 2019).

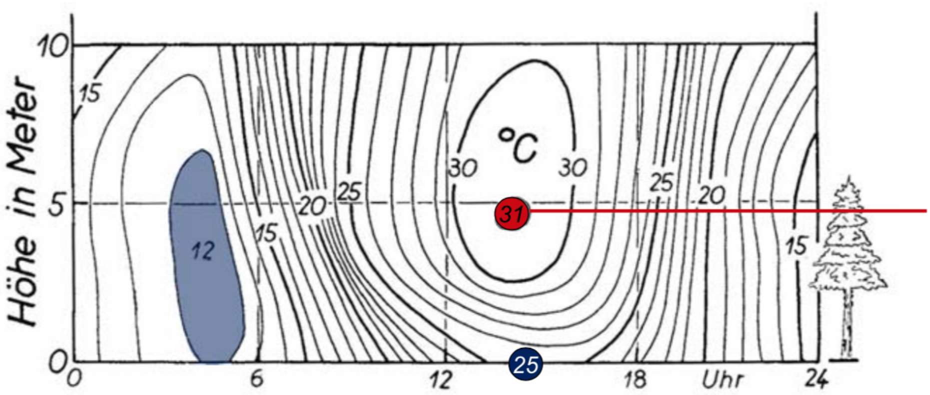

Figure 10: Diurnal mean temperature distribution with height of a young spruce forest taken from Prof. Dr Helmut Schume's presentation for heat budgets of forests (Schume, 2019). Coloured blue is the minimum and red the maximum temperature during a cloudfree day.

As WRF's 2 m temperature $T2$ is calculated with the skin temperature TSK and sensible heat flux HSX (see Equation 1), it is obvious that this is not the same 2 m temperature which one may experiences while walking through a forest. The skin temperature TSK would in this case be the temperature on top of the forest canopy. Thus the model's 2 m temperature represents the temperature 2 m above the forest top.

4.6.1 Alluvial Forests

The alluvial forest develops close to a river like the Danube where the area is flooded regularly and gets supplied with new soil and nutrients. The groundwater, which is connected to the level of the river, has thus significant influence on the alluvial forest.

The forest can be classified into a soft and a hard alluvial forest. The soft alluvial forest starts next to the river, even on the river's gravel bars, with willows that stabilise the ground and accumulate mud and loam. As soon as there is enough mud, sand and loam, poplar trees are able to establish in this humus lacking areas. Further away from the river but still in the soft part of the alluvial forest, alder and ash trees are present because they are also able to handle the flooding of the area.

The hard part of the alluvial forest starts where the flooding happens rarely and only in extreme situations. The groundwater level is almost constant and the soil becomes more rich in humus. In this area hardwood trees like oak, elm and maple tree are able to establish (Jelem, 1974).

4.7 Approach

As described in Section 4.6.1 an alluvial forest features a continuous connection to groundwater. In contrast to a forest without a connection to groundwater the alluvial forests vegetation should not get into water stress and thus water should still be able to evaporate during a heatwave. Because of this ongoing evaporation, the 2 m temperature which represents the temperature 2 m above the forest canopy as described in Section 4.6, should be lower than in the same forest without groundwater connection during a heatwave. This applies also to irrigated vegetation with the difference that this is a vegetation with root's that does not reach into depths where groundwater can be found. Hence, it also does not get into water stress because it gets irrigated and the irrigation usually happens from above.

In the NOAH land surface scheme the soil is divided into four layers. Different vegetation types have different root lengths. The roots of a tree from a deciduous broadleaf forest reach deep into the ground and can be found in all four layers of the model's soil. As there is no option for groundwater in the NOAH land surface model, the soil moisture content of layer three and four are set to $0.9\,m^3/m^3$ which means that they are filled with water even over their field capacity. The water which ca not be contained by the soil layer will be lost as runoff.

To simulate irrigation the soil moisture content of the second layer is also set to $0.9\,m^3/m^3$. Thereby the influence of the first layer's evapotranspiration is prevented while the vegetation's roots growing on cropland are still saturated.

To investigate the difference between irrigated and non irrigated situations and forests with and without groundwater connection, seven simulations are generated. The characteristics of those simulations are described in detail in Section 4.8.

The simulation time period starts with 05.08.2015 until 13.08.2015 and captures a heatwave in August 2015, see `https://www.zamg.ac.at/cms/de/klima/news/hitzewellen-2015-eines-der-extremsten-jahre-der-messgeschichte`.

Only days without clouds are of interest because clouds would interfere with the effects between surface and atmosphere. On basis of the models incoming solar radiation the days 08.08.2015, 09.08.2015 and 12.08.2015 were found to be cloudless. To see the differences in the simulations daily mean diurnal temperature and fluxes graphs are calculated. Two dimensional areal plots of these parameters and their difference to simulation REF are also calculated and will be presented in Chapter 5.

4.8 Scenarios

Table 6: WRF simulation scenarios and their modifications. The reference scenario REF is the same as in the Urbania project.

Name	Modification
REF	No modification
AU	Alluvial forest's SMC is set to 0.9 in layer three and four
REAL	Alluvial forest's SMC is set to 0.9 in layer three and four, irrigated cropland's SMC is set to 0.9 in layer two
IRR	Alluvial forest's SMC is set to 0.9 in layer three and four, All cropland's SMC is set to 0.9 in layer two
DRY	SMC of every landuse category is set to wilting point
WET	SMC of every landuse category is set to 0.9
AU_RS60's	Alluvial forest's SMC is set to 0.9 in layer three and four, stomatal resistance of alluvial forest is set to 60 1/s

To investigate the influence of modified soil moisture content (SMC), seven scenarios were created, see Table 6. The same reference scenario REF used in the Urbania project is used in this work to compare the other six modified scenarios to.

Alluvial forests are usually close to rivers and are connected to the groundwater. To simulate the groundwater for the AU scenario, the soil moisture content is set to $0.9\,m^3/m^3$ in layer three and four for WRF's landuse category USGS 11 "decidious broadleef forest". It also has to be inside the area Nationalpark Donauauen and in the alluvial forests around Tulln to be modified. To determine this area shapefiles were downloaded from `https://www.data.gv.at/katalog/dataset/nationalpark-donauauen-zonen`.

The scenarios DRY and WET are used to determine the model's sensitivity regarding modifications of the soil moisture content to the possible minimum and maximum of the soil. Thus the soil moisture content in all soil layers of simulation DRY was set bellow the wilting point, in example below $0.1\,m^3/m^3$, with the exact value depending on the soil type. In simulation WET all layer's soil moisture content has been set to $0.9\,m^3/m^3$.

To determine which of the cropland is irrigated for the REAL scenario, Dr. Francesco Vuolo from the Institute of Geomatics of the University of Natural Resources and Life Science provided a geotiff file matching domain three where irrigated land is classified with 1 and non irrigated land with 0. Based on this information, the affected landuse categories are set from cropland to irrigated cropland and additionally the soil moisture content in layer two is set to 0.9 m^3/m^3. The alluvial forest's soil moisture content was modified according to the AU scenario.

In the IRR scenario all cropland is simply set to be irrigated cropland with a changed soil moisture content of 0.9 m^3/m^3 in layer two. Again, the alluvial forest's soil moisture content was modified according to the AU scenario.

For scenario AU_RS60 a new category *Alluvial Forest*, based on category USGS 11 "deciduous broadleef forest", was created. These two landuse categories only differ in the modified stomatal resistance RS which is set to 60 1/m in the new category instead of 100 1/m. The soil moisture content in layer three and four of this category is also set to 0.9 m^3/m^3 to simulate groundwater according to the AU scenario.

5. Results

In this chapter the outputs of the scenarios described in Section 4.8 are compared to the reference scenario REF to investigate wether the scenarios deliver the expected effects and changes in certain meteorological parameters.
Figures of mean diurnal surface energy fluxes, 2 m temperature and skin temperature are calculated as well as two dimensional plots of the daily mean 2 m temperature or daily mean latent heat flux.

5.1 Scenario REF

As already mentioned in Section 4.8 scenario REF is the same reference scenario as in project Urbania. Its purpose is to be a reference for the other scenarios where changes are made in the initialised soil moisture content and the parameters of the land use category (scenario AU_RS60) and thus allow to illustrate which parameters are affected and in which way.

5.2 Scenario AU

The connection of a forest to groundwater has a major impact on the surface exchange fluxes as can be seen in Figure 11. In its left plot are the diurnal surface fluxes displayed while in the plot to the right the diurnal skin temperature and 2 m temperature are shown. The graphs are only calculated for the alluvial forest enclosed by the green contours in Figure 2.
The mean maximum of the diurnal latent heat flux LH occurs in scenario REF and AU around 11 UTC. Due to the connection to groundwater its value increases from scenario REF to AU by about 100 W/m^2. The diurnal sensible heat flux HFX decreases by the same amount with its mean maximum reached also around 11 UTC. A significant impact on the diurnal ground flux $GRDFLX$ can not be obtained.

Those changes can also be seen in the diurnal skin temperature TSK. Its peak is reached around 12 UTC with 38.5 °C which is around 2 °C lower than in the reference scenario. During nighttime it is only slightly colder, about 0.1 °C compared to scenario REF. Hence the impact on the diurnal 2 m temperature $T2$ is modest with decreased values during the day of about 0.5 °C.

Figure 12 shows the difference in the daily mean 2 m temperature between scenario AU and REF. The region of the alluvial forest with connection to groundwater is clearly visible because it is 0.25 to 0.5 °C cooler in the daily mean 2 m temperature compared to its surrounding.

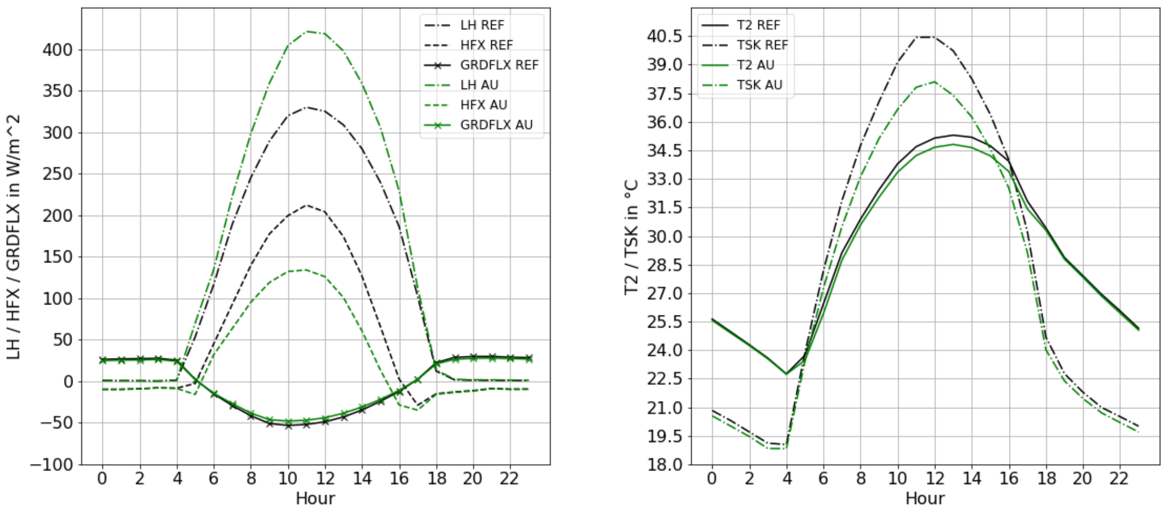

Figure 11: Mean diurnal fluxes and temperatures of scenario AU (green) compared to scenario REF (black) for selected cloudfree days.

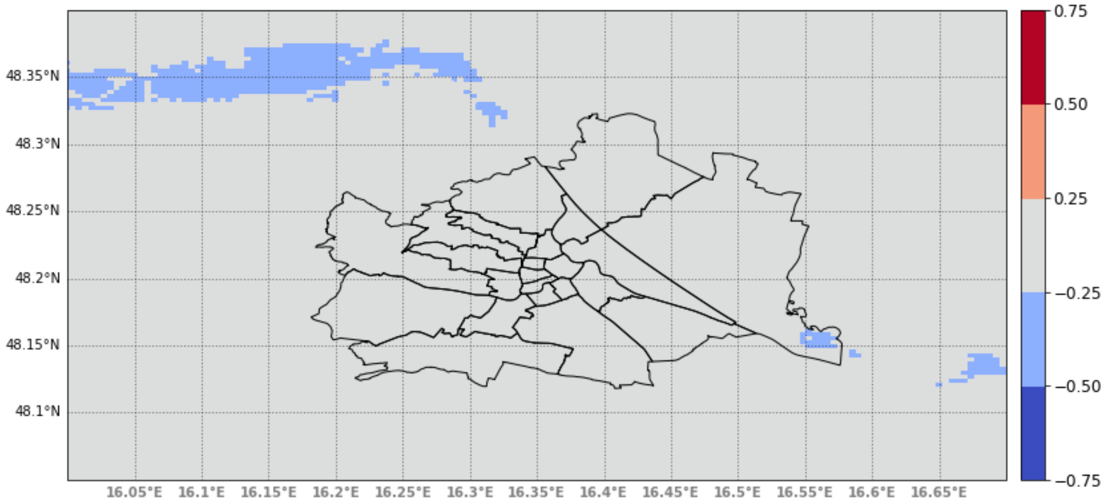

Figure 12: Difference in mean daily 2 m temperature between scenario AU and REF for selected cloudfree days.

5.3 Scenario DRY - WET / Model Sensitivity

As mentioned in Section 4.8 the scenarios DRY and WET shall illustrate the model's sensitivity and maximum possible effects regarding modifications in its initialised soil moisture content.

The domain's diurnal surface fluxes shown in the left plot of Figure 13 exibit the expected behavior. While WET's diurnal latent heat flux LH reaches its mean maximum of 490 W/m^2 at 11 UTC the diurnal latent heat flux LH of scenario DRY completely disappears. On the other hand, DRY's diurnal sensible heat flux HFX reaches the same mean maximum value as WET'S diurnal latent heat flux LH and simultaneously WET's diurnal sensible heat flux HFX has its mean maximum value of 70 W/m^2 around 9 UTC. As there is no latent heat flux LH in scenario DRY it's diurnal ground flux $GRDFLX$ absolute values are generally lower during day and night compared to scenario WET. This lower absolute values of the ground flux can be explained by the remaining sensible heat flux HSX of scenario WET which is therefore compensated by the ground flux as equation 3 demands.

The effects in the diurnal surface fluxes above explained and their impact are also obtained in the diurnal skin and 2 m temperature. During daytim the mean maximum of the diurnal skin temperature TSK of scenario DRY reaches 46.3 °C while scenario WET produces a mean maximum of 34.5 °C, leaving a difference of 12.2 °C. The mean maximum in the diurnal 2 m temperature shows a difference of 2.8 °C during daytime. This mean maximum is reached one hour later at 13 UTC in scenario WET compared to scenario DRY.

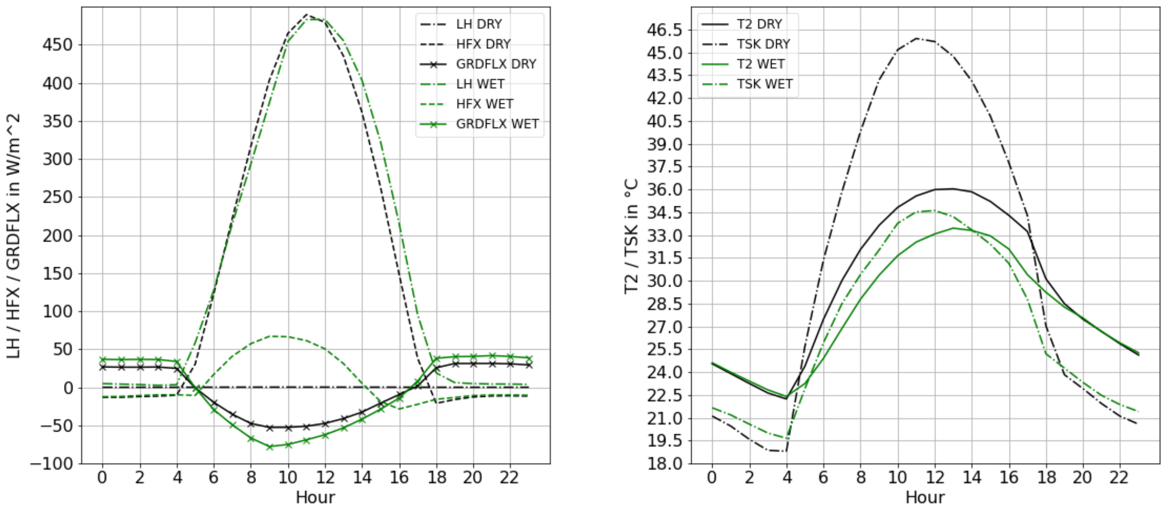

Figure 13: Mean diurnal fluxes and temperatures of scenario WET (green) compared to scenario DRY (black) for selected cloudfree days.

Figure 14 shows the difference in the daily mean latent heat flux LH between the scenarios DRY and WET. Significant differences in areas with forests like the Wienerwald and along the danube river with its alluvial forests are observed, with the biggest difference being up to 220 W/m^2.

Differences from 20 to 60 W/m^2 can be seen in the city of Vienna and no differences at all above the Danube river and small lakes around Vienna.

The same pattern appears in the daily mean 2 m temperature, displayed in Figure 15, with the biggest differences of up to 2.25 °C also occurring in forests and cropland. In the city of Vienna and generally in dense urban regions, above the Danube river and above small lakes the difference in 2 m temperature is insignificant.

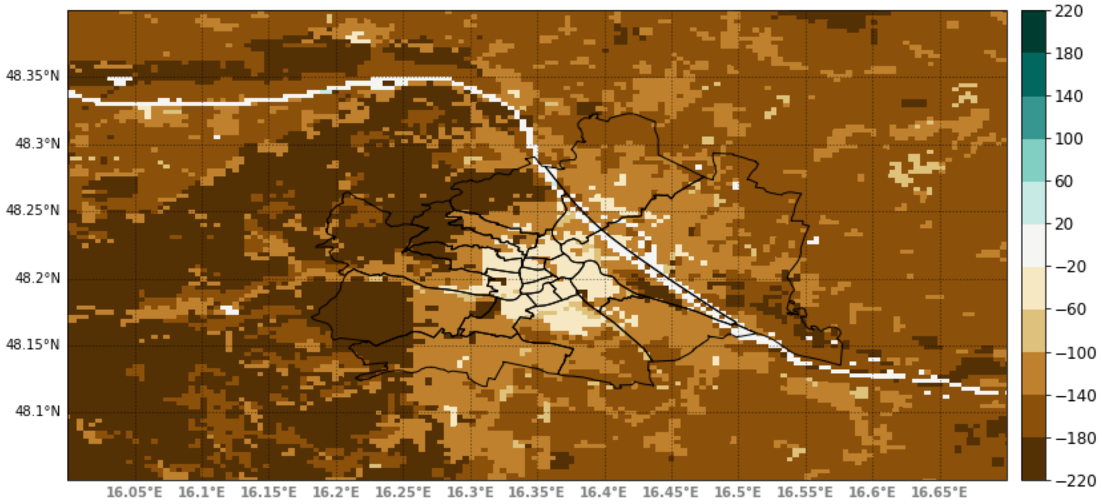

Figure 14: Difference in mean daily surface latent heat flux between scenarios DRY and WET for selected cloudfree days.

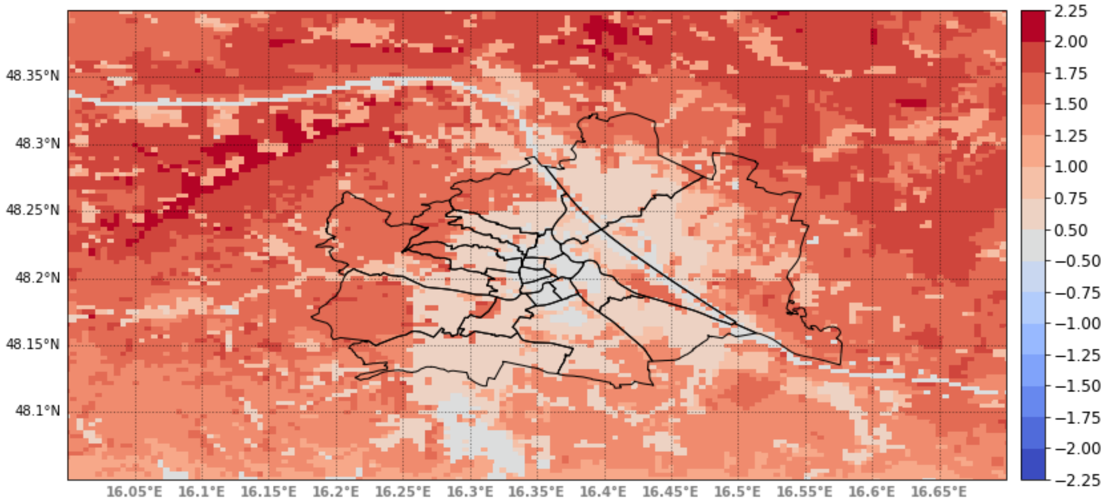

Figure 15: Difference in mean daily 2 m temperature between scenarios DRY and WET for selected cloudfree days.

5.4 Scenario IRR

5.4.1 Cropland

In scenario IRR the soil moisture content in layer two of all of the domain's cropland was set to 0.9 m^3/m^3 to simulate irrigation. For the graphs in Figure 16 all areas with landuse category irrigated cropland were used to illustrate the influence of irrigation in this area.

The mean maximum of the diurnal latent heat flux LH of scenario IRR increased by 200 W/m^2 to a mean maximum of 430 W/m^2 at 12 UTC compared to the reference scenario REF. The

diurnal sensible heat flux decreased to a mean maximum of 70 W/m^2 and also shifted its occurrence by 1 hour to 10 UTC. The diurnal latent and sensible heat flux for cropland in the REF scenario are showing almost the same development and are reaching their mean maximum with 230 W/m^2 and 250 W/m^2 around 11 UTC.
During nighttime the diurnal latent heat flux of scenario WET is slightly higher than its opponent in scenario REF. The diurnal ground flux of both scenarios also develop very similar but with slightly higher absolute values in scenario WET.

The IRR's mean maximum of the cropland's diurnal skin temperature gets reduced by about 3.7 °C, from 40.5 °C to 36.8 °C. Its diurnal 2 m temperature $T2$ shows somewhat higher values during nighttime than in scenario REF and lower values during daytime with a difference in the mean maximum of 1.5 °C reduced from 35.5 °C in scenario REF to 34 °C in IRR.

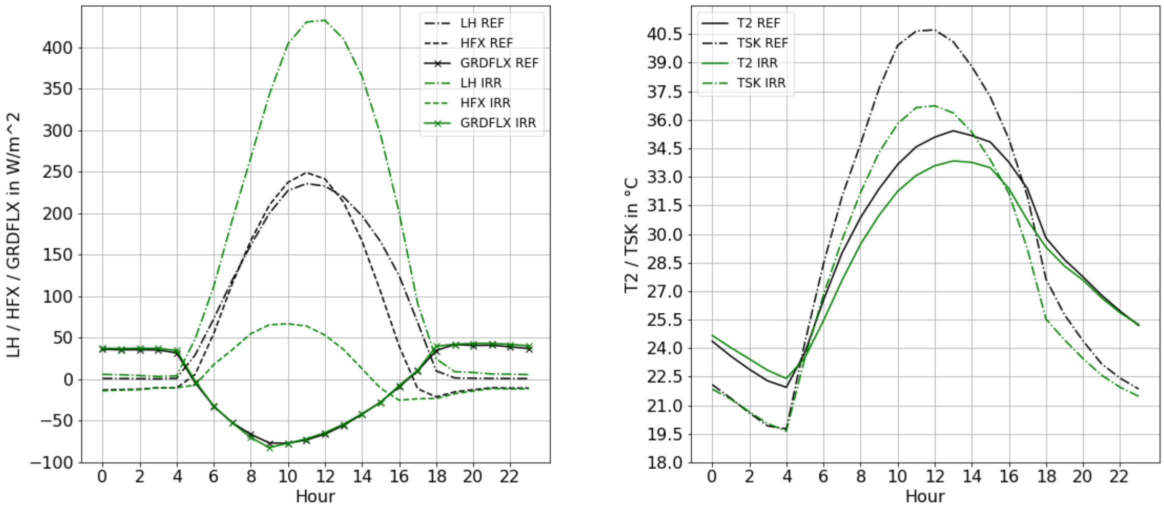

Figure 16: Mean diurnal fluxes and temperatures of scenario IRR (green) compared to scenario REF (black) ONLY for domain's landuse irrigated cropland for selected cloudfree days.

The difference in the daily mean 2 m temperature in the whole domain, shown in Figure 17, is with 1.0 to 1.25 °C the highest in the irrigated croplands. In the alluvial forest close to the Danube river, where the soil moisture content is set to 0.9 m^3/m^3, the difference is lower than over cropland with values from 0.25 to 0.75 °C.

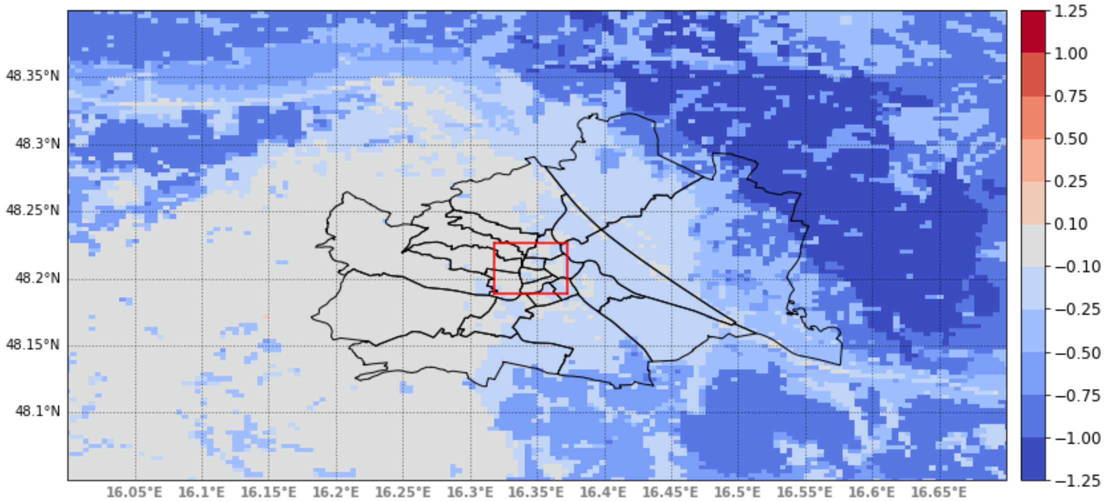

Figure 17: Difference in mean daily 2 m temperature between scenarios IRR and REF for selected cloudfree days. The red rectangle frames the area regarding the analyses for the influence on the city of Vienna.

5.4.2 City of Vienna

To investigate wether the artificial irrigation created by changing the initialized soil moisture content in soil layer two, has an impact on the city of Vienna, the area inside the red rectangle in Figure 17 is used to compare between scenario IRR and REF. The same diurnal fluxes and temperatures are calculated but only for the area inside the red rectangle for both scenarios, REF and IRR.

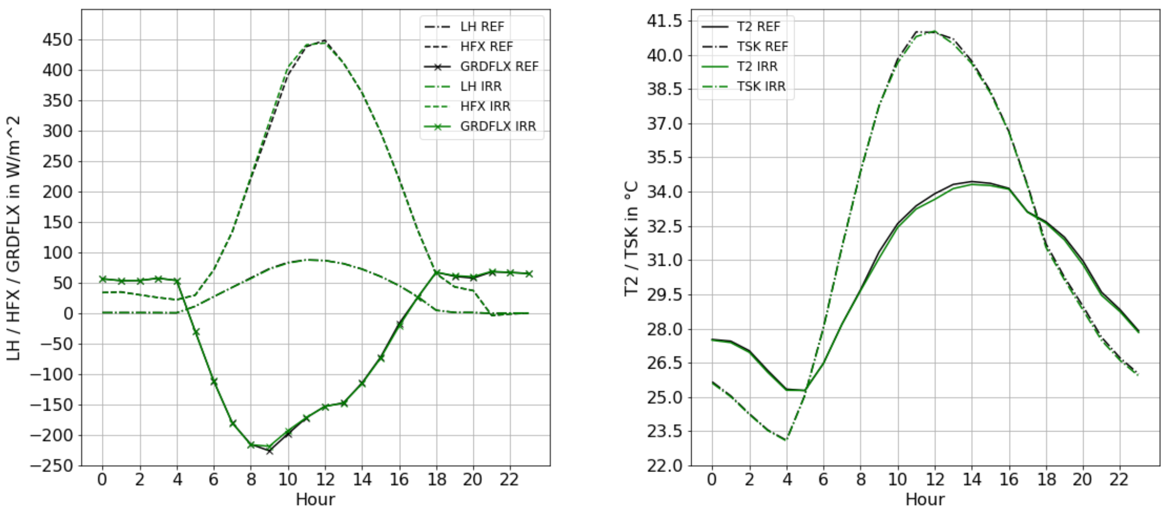

Figure 18: Mean diurnal fluxes and temperatures of scenario IRR (green) compared to scenario REF (black) ONLY for the city of Vienna in the area framed by the red rectangle in Figure 17 for selected cloudfree days.

As shown in Figure 18, there is almost no influence on the city of Vienna in the diurnal skin temperature. The diurnal 2 m temperature shows slightly lower values between 8 and 14 UTC. This difference reaches its mean maximum between 11 and 13 UTC. All in all the mean difference for the three chosen days for this area was calculated to be 0.09 °C.

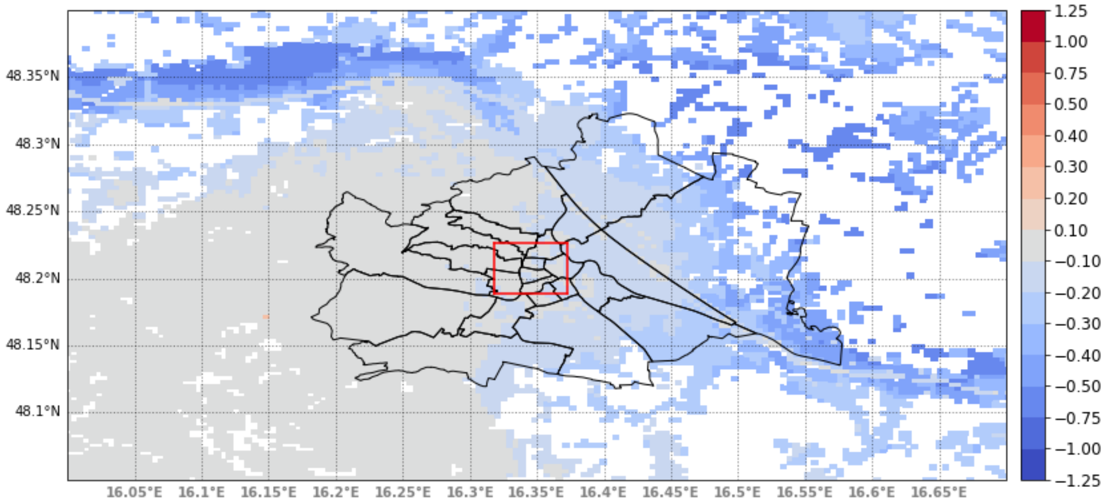

Figure 19: Difference in mean daily 2 m temperature between scenarios IRR and REF for selected cloudfree days. The red rectangle frames the area regarding the analyses for the influence on the city of Vienna. White areas show the domain's landuse irrigated cropland with removed values to display the influence on the surrounding.

Still, as shown in Figure 19, the outlying districts of Vienna in the northeast facing cropland dominated rural areas, namely Donaustadt and Floridsdorf, experience lower values in the daily mean 2 m temperature. The white areas in Figure 19 mark the landuse of irrigated cropland and were set to zero to investigate wether the irrigation influences areas around it. Starting in those two districts at the borders to the irrigated cropland, the areas closeby show up to 0.5 °C lower values in the daily mean 2 m temperature. Facing towards the inner city, marked by a red rectangle, every three grid points, corresponding to a distance of around 1 km the temperature drops about 0.1 °C compared to the REF scenario. This temperature drop can even be observed in the district Brigittenau which is next to Floridsdorf and touches the right upper corner of Figure's 19 red rectangle.

5.5 Scenario REAL

As described in Section 4.8, the real irrigation of the cropland around Vienna was determined according to the information provided by Dr. Francesco Vuolo. For Figure 20 the parameters for all cropland, irrigated and non irrigated, are compared to investigate the effects caused by the changed soil moisture content of soil layer two on all of the cropland region.

An increase of about 20 W/m^2 in the mean maximum of the diurnal latent heat flux LH to 250 W/m^2 can be obtained in scenario REAL compared to REF. At the same time the mean maximum of the diurnal sensible heat flux HFX decreases by about 20 W/m^2 from 250 to 230 W/m^2 in scenario REAL compared to REF. In the diurnal ground flux $GRDFLX$ no changes are noticed.

During daytime a reduction in the diurnal skin as well as in the 2 m temperature between scenario REAL and REF for the whole area of irrigated and dry cropland is observed. The difference in the mean maximum of the diurnal skin temperature is about 0.2 °C and is reduced from 40.6 °C in scenario REF to 40.4 °C in scenario REAL. The diurnal 2 m temperature's mean maximum is reduced from 35.5 °C in REF to 35.4 °C in scenario REAL.

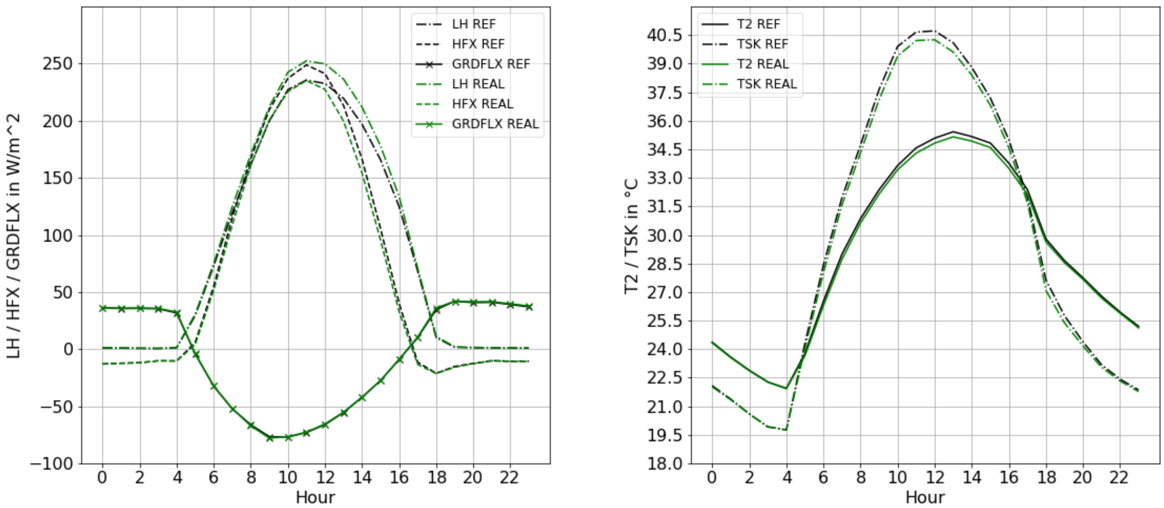

Figure 20: Mean diurnal fluxes and temperatures of scenario REAL (green) compared to scenario REF (black) for all cropland landuse categories in domain three for selected cloudfree days.

Figure 21 shows that the changes in the daily mean 2 m temperature are of local nature and stick to cropland with simulated irrigation. In those places the difference in the daily mean 2 m temperature can range from 0.5 up to 1.0 °C.

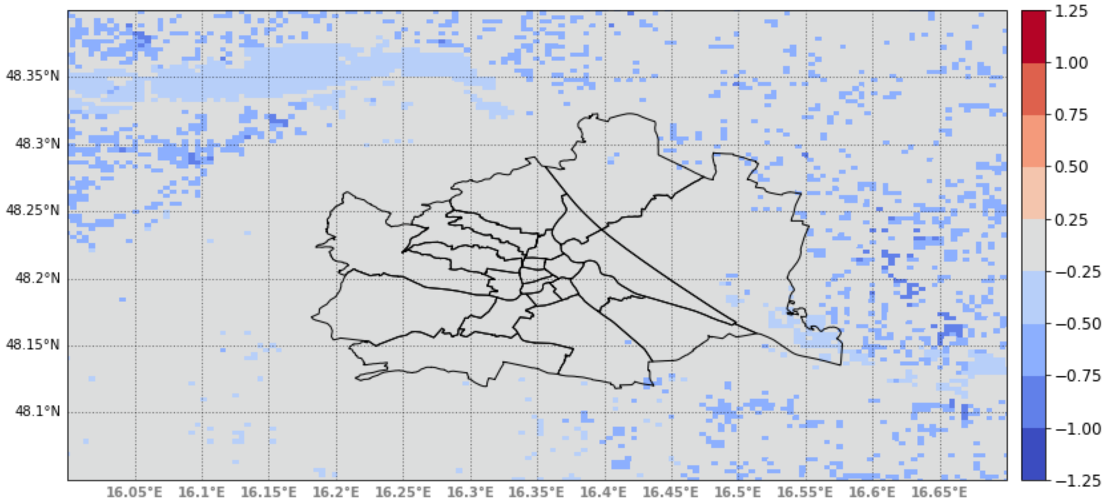

Figure 21: Difference in mean daily 2 m temperature between scenarios REAL and REF for selected cloudfree days.

5.6 Scenario AU_RS60

A new landuse category for alluvial forests was created with a reduced stomatal resistance to 60 1/s as described in Section 4.8. This section shows results of scenario AU_RS60 and compares them to scenario REF and AU to illustrate the impact caused by the change in the vegetation's stomatal resistance.
For Figures 22 and 25 only the areas of alluvial forests, marked with green contours in Figure 2 are used to calculate the diurnal surface fluxes and temperatures as well as the two dimensional plots of certain meteorological parameters and their differences.

5.6.1 Comparison to REF

An increase of about 150 W/m^2 in AU_RS60's mean maximum in the diurnal latent heat flux LH from 330 W/m^2 in scenario REF to 480 W/m^2 can be observed. The diurnal sensible heat flux's mean maximum HFX in scenario AU_RS60 is reduced by 120 W/m^2 from 210 W/m^2 in scenario REF to 90 W/m^2 in scenario AU_RS60. The remaining 20 W/m^2 (due to energy balance demanded by Equation 3) can be attributed to the diurnal ground flux $GRDFLX$ where the absolute value of the mean maximum during daytime is reduced from 50 W/m^2 in scenario REF to 30 W/m^2 in scenario AU_RS60.

The changes in the surface fluxes take effect as the diurnal skin temperature's maximum is reduced by 4.3 °C from 40.5 °C in scenario REF to 36.2 °C in scenario AU_RS60. Additionally, the diurnal skin temperature is constantly reduced throughout the whole night by about 0.2 °C in scenario AU_RS60 compared to REF. The effects in the diurnal 2 m temperature can still only be seen during daytime where scenario AU_RS60's mean maximum is reduced from 35.3 °C in REF to 34.5 °C.

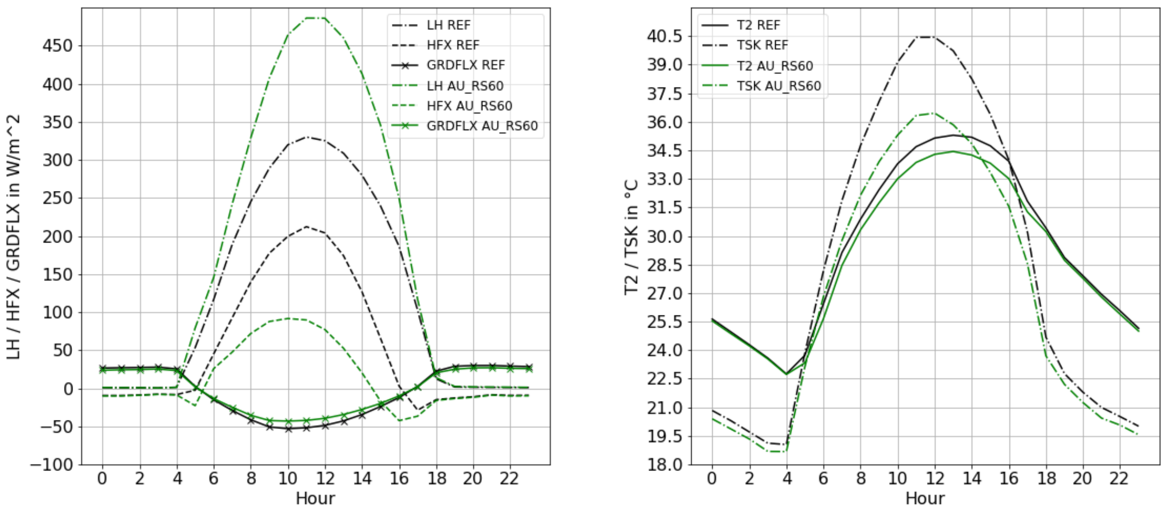

Figure 22: Mean diurnal fluxes and temperatures of scenario AU_RS60 (green) compared to scenario REF (black) for selected cloudfree days.

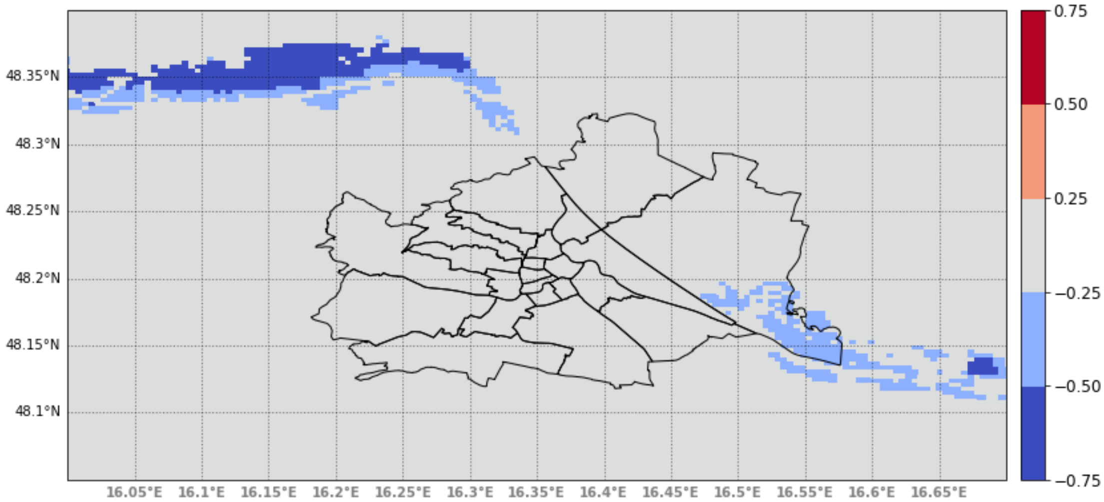

Figure 23: Difference in mean daily 2 m temperature between scenarios AU_RS60 and REF for selected cloudfree days.

The difference in the daily mean 2 m temperature shown in Figure 23 ranges from 0.25 to 0.75 °C with the highest difference observed in the Tullner Feld north west of Vienna.

5.6.2 Comparison to AU

The AU_RS60's mean maximum of the diurnal latent heat flux LH increases by 60 W/m^2 compared to scenario AU and reaches about 490 W/m^2. Hence the scenarios mean maximum in the diurnal sensible heat flux HFX is reduced by 50 W/m^2 to 90 W/m^2 with a shift in time from 11 UTC to 10 UTC. The remaining 10 W/m^2 to meet the demanded balance of Equation 3 are covered by the diurnal ground flux as its mean maximum decreases by 10 W/m^2 in absolute terms.

The diurnal skin temperature shows a difference in its mean maximum between the two scenarios of about 1.5 °C and is reduced to 36.4 °C in scenario AU_RS60. The effect in the diurnal 2 m temperature between AU_RS60 and AU is a reduction of 0.3 °C, from 34.7 to 34.4 °C in the mean maximum.

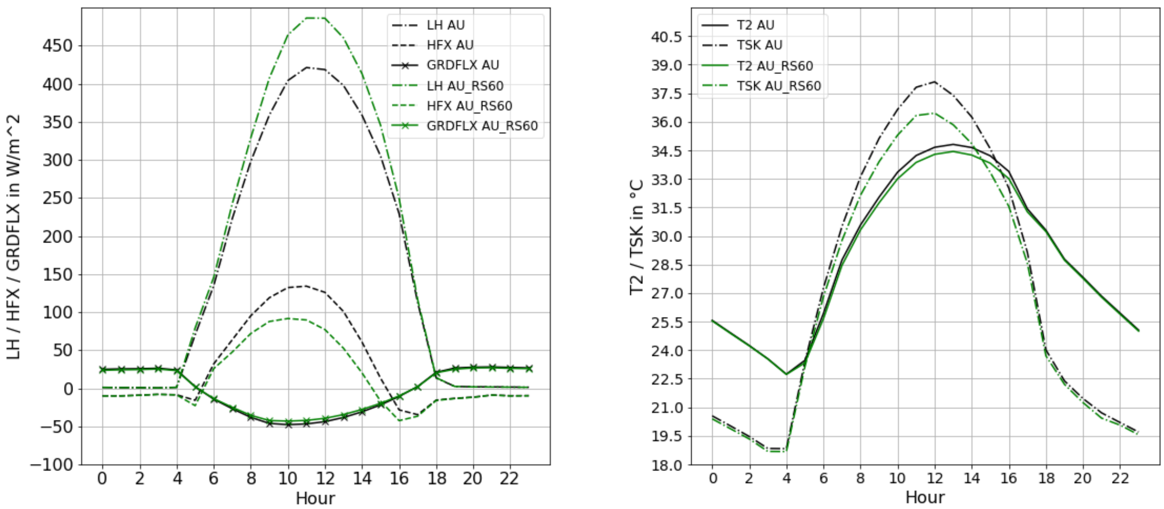

Figure 24: Mean diurnal fluxes and temperatures of scenario AU_RS60 (green) compared to scenario AU (black) for selected cloudfree days.

Again, the biggest difference in the daily mean 2 m temperature can be found in the Tullner Feld's alluvial forest in the north west of Vienna with about 0.3 °C lower values in scenario AU_RS60. In some spots in the Nationalpark Donauauen in the east of Vienna, the difference also reaches up to 0.3 °C, but the majority of this area shows a difference between 0.1 and 0.2 °C.

The impact of the reduced stomatal resistance in the new category AU_RS60 is characterised by a maximum of 0.3 °C in the daily mean 2 m temperature compared to scenario AU.

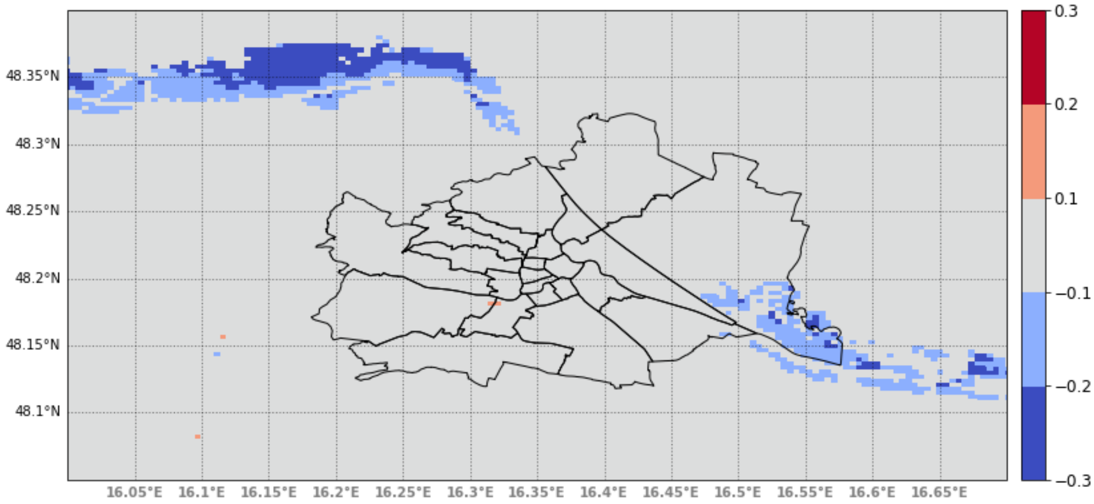

Figure 25: Difference in mean daily 2 m temperature between scenarios AU_RS60 and AU for selected cloudfree days.

5.7 Postprocessing WRF-TEB's Output

To prevent missunderstandings when presenting results to clients, post processing the 2 m temperature output of WRF-TEB's simulations with an algorithm that reduces the temperature according to the type of vegetation of the landuse category, should be considered. Especially for vegetation with a high canopy, large differences in the maximum of the 2 m temperature can occur (for details see Section 4.6).

Figure 26 shows an example for such a plot. To produce this figure, a simple approach was performed. In areas with landuse category forest, the temperature difference at midday, shown in Figure 11, was subtracted from WRF-TEB's output. The result is the mean maximum 2 m temperature with the climatology of a forest being taken into account and thus a more realistic 2 m temperature can be presented.

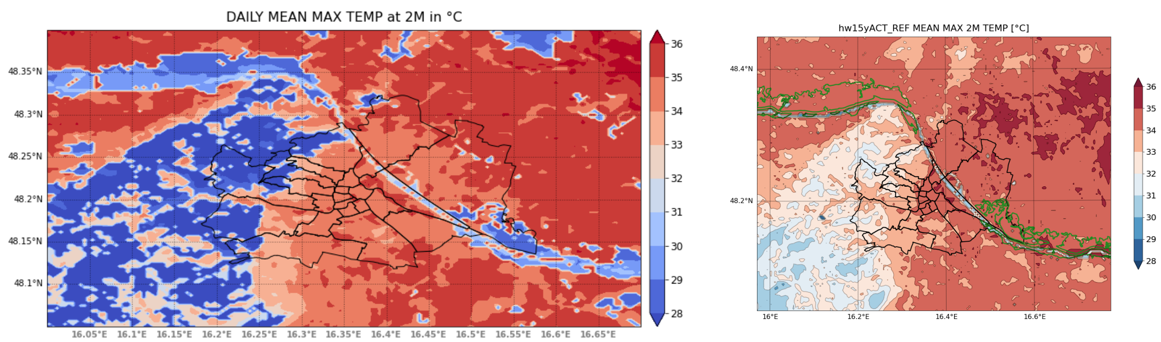

Figure 26: Mean of the selected cloud free days for each grid cell for the daily 2 m maximum air temperature under consideration of the climatology inside a forest. For comparison next to it Figure 2 with the mean maximum 2 m temperature from the Urbania project.

5.8 Summarised Results

Table 7 lists the differences between the generated scenarios with modifications in the soil moisture content and the REF scenario. The displayed values are calculated only for the areas where modifications took place. For the scenarios IRR and REAL this means all cropland of domain three, for the scenarios AU and AU_RS60 the alluvial forest connected to the Danube river framed by the green contours in Figure 2.

Table 7: Differences between the scenarios and the REF scenario. Values are calculated for the areas of interest meaning the alluvial forest for scenarios AU and AU_RS60 and cropland for scenarios IRR and REAL.

	AU	AU_RS60	IRR	REAL
max. 2 m temperature [°C]	-0.5	-0.8	-1.5	-0.1
max. skin temperature [°C]	-2.0	-4.3	-3.7	-0.2
max. latent heat flux [W/m^2]	100	120	200	20
max. sensible heat flux [W/m^2]	-100	-120	-180	-20
max. ground flux [W/m^2]	0	0	-20	0

6. Discussion and Conclusion

In this chapter the questions revealed from project Urbania, stated in Section 1.3, are discussed with the help of this work's results.

How can the initial soil moisture input parameter be modified to elucidate the effects of irrigation or an alluvial forest?

The most important properties of an alluvial forest are its connection to groundwater and therefore its continuous ability of transpiration also during heatwaves.

The data used in this work to initialize the soil moisture content do not contain groundwater in the areas of alluvial forests. As the NOAH land surface model does not have an option for irrigation or groundwater, it was found to be most efficient to modify the soil moisture content in the *geo_em** files which are produced by WPS to initialise WRF. This approach was found to be sufficient for the length of this work's simulation. For longer simulations a different approach, where the irrigation happens periodically during the simulation, would have to be considered because the initial soil moisture content, especially in the upper layers, would eventually get completely evapotranspirated.

How does the soil moisture content influence the 2 m temperature and evapotranspiration?

As shown by scenario DRY and WET, soil moisture has a major impact on the results of WRF-TEB's simulations. It changes the balance of the surface energy fluxes from Equation 3, shown in Figures 14, 15 and 13, which has direct influence on the skin temperature and on the 2 m temperature.

In this work's domain three, the difference for the mean maximum of the diurnal 2 m temperature between completely dry and all wet during daytime reaches almost 3 °C. The difference in the diurnal skin temperature's mean maximum even reaches 11.5 °C. This can have a major impact on the environment or the human body especially in extreme events like the August 2015 heatwave.

How will the modified input parameters effect the temperature in these areas? - Alluvial Forest

Scenario AU delivered results on how big the impact of groundwater on the model's broadleaf forests is. While its influence on the mean maximum of the diurnal skin temperature is about 2.5 °C, the mean maximum of the diurnal 2 m temperature only gets reduced by 0.5 °C.
The reduction in the forests stomatal resistance delivered a further decrease of about 0.3 °C in the diurnal 2 m temperature during daytime for a simulation period of one week.

All in all this does not seem to be a big difference, however, with a longer ongoing heatwave the impact of a connection to groundwater might increase even further.

One has also to consider that the model was initialised with too high values in the soil moisture as Figure 9 shows. The influence of this wet bias can be seen in figure 8 as the minimum and maximum of the diurnal 2 m temperature is not simulated correctly.
For further simulations it would be of interest to use the calculated soil moisture content of a regional agricultural model like ARIS to initialize WRF.

How will the modified input parameters effect the temperature in these areas? - Cropland

As already mentioned above the mean maximum of the diurnal 2 m temperature of forests was reduced by about 0.5 °C by adding groundwater to the soil. A further reduction of the stomatal resistance to 60 1/s in simulation AU_RS60 led to a decrease of 0.8 °C compared to simulation REF.

Simulation REAL shows a real case irrigation scenario. The impact of irrigation on cropland can be up to 1.25 °C reduction in the mean 2 m temperature and sticks to the areas with irrigated cropland with areas without irrigation inbetween. The comparison between all cropland, irrigated and non irrigated, shows a rather low impact with just 0.1 °C reduction in the mean maximum of the diurnal 2 m temperature because there is much less irrigated cropland then non irrigated cropland.

In the artificial scenario IRR where all cropland in domain three is irrigated, the reduction in the mean 2 m temperature reaches 1.5 °C in the irrigated areas.
Scenario IRR was also used to answer the following question.

Will the created effects also influence the temperature in Vienna?

Even the artificial scenario IRR with irrigation of all cropland in domain three showed only little impact on the daily mean 2 m temperature of the inner city of Vienna, marked by a red rectangle in Figure 17 (reduction of 0.09 °C).

Even though scenario IRR's influence on the daily mean 2 m temperature of Vienna's inner city is negligible, a reduction of up to 0.5 °C in outlying districts like Donaustadt and Floridsdorf and 0.1 °C even in Brigittenau (see Figure 19) was obtained.

Is it an improvement to create a new landuse category for alluvial forests?

A new landuse category was created by reducing the stomatal resistance of the landuse category for broadleaf forests. This modification yields a reduction of up to 0.3 °C in the daily mean 2 m temperature in this works simulation. In terms of creating a realistic climatology for the inside of a forest, this option is not an improvement.

A closer look at Equation 1 reveals that the 2 m temperature is calculated with the skin temperature TSK and the sensible heat flux HFX. Therefore, one has to keep in mind that WRF's 2 m temperature is always above the skin of the landuse. Regarding a forest this means that it is located 2 m above the treetop which in that case is not the 2 m temperature we experience while taking a stroll in the forest.

Hence, in terms of heatwaves, the post processing of WRF-TEB's 2 m temperature output has proven to provide plots that are more reasonable when presented to costumers who are not

familiar with the specific calculation of certain parameters in WRF-TEB.
In this work only a very simple approach was used. The maximum difference between the top of a forest and the temperature inside of the forest during a sunny summer day was subtracted from the maximum 2 m temperature. A more complex algorithm considering more variables such as intensity of incoming solar radiation, the julian day or different types of vegetation would be of great interest.

In conclusion, it can be said that by changing the initialised soil moisture content the climatology inside a forest can not be reproduced. The modification of the stomatal resistance also does not deliver the desired reduction in temperature.
Irrigation reduces the mean 2 m temperature by up to 1.5 °C but only in the designated areas as the real-case scenario REAL illustrates. To also affect areas around the irrigated cropland, a vast area of irrigation is necessary which is not realistic and uneconomical regarding water consumption.

It would be of great interest to investigate how the modification of the soil moisture content influences the production of rain and formation of clouds because those effects also have a major impact on skin and 2 m temperature.

For further projects it would be interesting to couple the TEB Model with the newer NOAH MP land surface model. MP stands for Multi Parametrisation and contains options for irrigation and groundwater. Additionally the type of crop can be chosen, with each crop having different properties. Instead of a flat two-dimensional approach like in the former NOAH land surface model, the NOAH MP land surface model uses a canopy approach with a top and bottom layer which enables the model to take into account shading effects and makes it possible to calculate proper surface energies and water transfer processes in the vegetation canopy (Niu et al., 2011).

Acknowledgment

First of all, I want to thank my supervisor Herbert Formayer fom the University of Natural Resources and Life Sciences for the great support and fast responses during the whole process. Secondly, I want to thank the Austrian Climate Research Programme (ACRP) who funded the Urbania project (ACRP number KR15AC8K12615) and made this master's thesis possible in the first place. I also want to express my gratitude towards ECMWF, Copernicus and ESA, Earthdata, NASA, NOAH and all other institutions with an open source credo who are laying the foundation with their free data or software for great and interesting research opportunities. A thank you goes out to my colleagues from the University of Natural Resources and Life Sciences for their inputs and technical support, especially to Dr. Francesco Vuolo and Dr. Josef Eitzinger. I would also like to thank my family whose, also financial, support over the past years made life much easier. A big thank you goes out to Julia Wind who helped me improving the linguistic quality and helped finding all the typos and grammatical mistakes. Last but not least I want to mention my colleagues and friends from university who made the time studying an exceptionally pleasant one.

Bibliography

, ????: arw version 3 modeling system user's guide. mesoscale&miscroscale meteorology division. national center for atmospheric research.

Best, M., A. Beljaars, J. Polcher, and P. Viterbo, 2004: A proposed structure for coupling tiled surfaces with the planetary boundary layer. *Journal of Hydrometeorology*, **5 (6)**, 1271–1278.

Bueno, B., G. Pigeon, L. Norford, K. Zibouche, and C. Marchadier, 2012: Development and evaluation of a building energy model integrated in the TEB scheme.

De Munck, C., A. Lemonsu, R. Bouzouidja, V. Masson, and R. Claverie, 2013: The GREENROOF module (v7. 3) for modelling green roof hydrological and energetic performances within TEB.

ECMWF, 2018: Set I - Atmospheric Model high resolution 10-day forecast (HRES). European Centre for Medium-Range Weather Forecasts, URL https://www.ecmwf.int/en/forecasts/datasets/set-i, accessed: June 2018.

Eitzinger, J., and Coauthors, 2016: Drought monitoring system for Austrian agriculture – AgroDroughtAustria (Final Scientific Report of project "AgroDroughtAustria" of the Austrian Climate Change Research Program). *BOKU-Met Report 25, ISSN 1994-4179. ISSN 1994-4187*, URL https://meteo.boku.ac.at/report/.

Ek, M., K. Mitchell, Y. Lin, E. Rogers, P. Grunmann, V. Koren, G. Gayno, and J. Tarpley, 2003: Implementation of Noah land surface model advances in the National Centers for Environmental Prediction operational mesoscale Eta model. *Journal of Geophysical Research: Atmospheres*, **108 (D22)**.

European Environment Agency (EEA), 2012: Corine land cover dataset 2012. European Environment Agency (EEA) under the framework of the Copernicus programme, URL https://land.copernicus.eu/pan-european/corine-land-cover/clc-2012, accessed: 23.05.2018.

Farr, T. G., and Coauthors, 2007: The shuttle radar topography mission. *Reviews of geophysics*, **45 (2)**.

Goret, M., V. Masson, R. Schoetter, and M.-P. Moine, 2019: Inclusion of CO2 flux modelling in an urban canopy layer model and an evaluation over an old European city centre. *Atmospheric Environment: X*, **3**, 100 042.

Greve, P., K. Warrach-Sagi, and V. Wulfmeyer, 2013: Evaluating soil water content in a WRF-Noah downscaling experiment. *Journal of applied meteorology and climatology*, **52 (10)**, 2312–2327.

Haiden, T., A. Kann, C. Wittmann, G. Pistotnik, B. Bica, and C. Gruber, 2011: The Integrated Nowcasting through Comprehensive Analysis (INCA) system and its validation over the Eastern Alpine region. *Weather and Forecasting*, **26 (2)**, 166–183.

Hirschi, M., and Coauthors, 2011: Observational evidence for soil-moisture impact on hot extremes in southeastern Europe. *Nature Geoscience*, **4 (1)**, 17–21.

Jelem, H., 1974: Auwalder der Donau in Osterreich. The bottomland forests of the Danube in Austria.

Klein Tank, A., and G. Können, 2003: Trends in indices of daily temperature and precipitation extremes in europe, 1946–99. *Journal of climate*, **16 (22)**, 3665–3680.

Kromp-Kolb, H., T. Lindenthal, and L. Bohunovsky, 2014: Österreichischer Sachstandsbericht Klimawandel 2014. *GAIA-Ecological Perspectives for Science and Society*, **23 (4)**, 363–365.

Lemonsu, A., V. Masson, L. Shashua-Bar, E. Erell, and D. Pearlmutter, 2012: Inclusion of vegetation in the Town Energy Balance model for modelling urban green areas.

Martilli, A., A. Clappier, and M. W. Rotach, 2002: An urban surface exchange parameterisation for mesoscale models. *Boundary-layer meteorology*, **104 (2)**, 261–304.

Masson, V., 2000: A physically-based scheme for the urban energy budget in atmospheric models. *Boundary-layer meteorology*, **94 (3)**, 357–397.

Masson, V., M. Bonhomme, J.-L. Salagnac, X. Briottet, and A. Lemonsu, 2014: Solar panels reduce both global warming and urban heat island. *Frontiers in Environmental Science*, **2**, 14.

Masson, V., C. S. B. Grimmond, and T. R. Oke, 2002: Evaluation of the Town Energy Balance (TEB) scheme with direct measurements from dry districts in two cities. *Journal of applied meteorology*, **41 (10)**, 1011–1026.

Meyer, D., and Coauthors, 2020: WRF-TEB: implementation and evaluation of the coupled Weather Research and Forecasting (WRF) and Town Energy Balance (TEB) model. *Journal of Advances in Modeling Earth Systems*, e2019MS001961.

Miao, S., F. Chen, M. A. LeMone, M. Tewari, Q. Li, and Y. Wang, 2009: An observational and modeling study of characteristics of urban heat island and boundary layer structures in beijing. *Journal of Applied Meteorology and Climatology*, **48 (3)**, 484–501.

Mitchell, K., 2005: The community Noah land-surface model (LSM).

Niu, G.-Y., and Coauthors, 2011: The community Noah land surface model with multiparameterization options (Noah-MP): 1. Model description and evaluation with local-scale measurements. *Journal of Geophysical Research: Atmospheres*, **116 (D12)**.

Oke, T. R., 1973: City size and the urban heat island. *Atmospheric Environment (1967)*, **7 (8)**, 769–779.

Pineda, N., O. Jorba, J. Jorge, and J. Baldasano, 2004: Using NOAA AVHRR and SPOT VGT data to estimate surface parameters: application to a mesoscale meteorological model. *International journal of remote sensing*, **25 (1)**, 129–143.

Rausch, J., 2012: Improvement of short term precipitation forecasts in the Alpine Region using WRF with 3DVAR RADAR Reflectivity and SYNOP assimilation. Ph.D. thesis, uniwien.

Rodell, M., and Coauthors, 2004: The global land data assimilation system. *Bulletin of the American Meteorological Society*, **85 (3)**, 381–394.

Schicker, I., D. A. Arias, and P. Seibert, 2016: Influences of updated land-use datasets on WRF simulations for two Austrian regions. *Meteorology and Atmospheric Physics*, **128 (3)**, 279–301.

Schoetter, R., V. Masson, A. Bourgeois, M. Pellegrino, and J.-P. Lévy, 2017: Parametrisation of the variety of human behaviour related to building energy consumption in the Town Energy Balance (SURFEX-TEB v. 8.2). *Geoscientific Model Development*, **10 (7)**, 2801.

Schume, H., 2019: Lecturenotes Waldklimatologie.

Seneviratne, S. I., D. Lüthi, M. Litschi, and C. Schär, 2006: Land–atmosphere coupling and climate change in europe. *Nature*, **443 (7108)**, 205–209.

Skamarock, W., J. Klemp, J. Dudhia, D. Gill, D. Barker, W. Wang, and J. Powers, 2005: A description of the Advanced Research WRF version 2. NCAR Tech. Tech. rep., Note NCAR/TN-4681STR.

Steppeler, J., G. Doms, U. Schättler, H. Bitzer, A. Gassmann, U. Damrath, and G. Gregoric, 2003: Meso-gamma scale forecasts using the nonhydrostatic model LM. *Meteorology and atmospheric Physics*, **82 (1-4)**, 75–96.

Tran, H., D. Uchihama, S. Ochi, and Y. Yasuoka, 2006: Assessment with satellite data of the urban heat island effects in Asian mega cities. *International journal of applied Earth observation and Geoinformation*, **8 (1)**, 34–48.

Trimmel, H., and Coauthors, 2019: Thermal conditions during heat waves of a mid-European metropolis under consideration of climate change, urban development scenarios and resilience measures for the mid-21st century. *Meteorologische Zeitschrift*.

Wang, Y., T. Haiden, and A. Kann, 2006: *The operational limited area modelling system at ZAMG: ALADIN-AUSTRIA*. Zentralanstalt für Meteorologie und Geodynamik.